Drag computation for incompressible flows with a Nitsche's type stabilization method

Daniela Capatina, Robert Luce, David Trujillo

Version of Record: https://www.sciencedirect.com/science/article/pii/S004578251930667X
Manuscript_7b21b57c44ac6c02aa7a1c64c23415c9

Drag computation for incompressible flows with a Nitsche's type stabilization method

Daniela Capatina[b,*], Robert Luce[b], David Trujillo[b]

[b] *LMAP & CNRS UMR 5142, University of Pau, IPRA BP 1155, Av. de l'Université, 64013 Pau, France*

Abstract

In this paper we study the drag error for the incompressible Navier-Stokes equations, satisfying a modified outflow condition allowing to take into account re-entrant flows, and approximated by conforming $(P_1)^2 \times P_1$ or $(Q_1)^2 \times Q_1$ finite elements. The numerical scheme uses a SUPG stabilization on the cells and a new Nitche's type stabilization on the whole boundary, with well-chosen non-linear stabilization parameters. We introduce a definition of the discrete drag which contains additional terms, resulting from the treatment of the non-linearity and from Nitsche's stabilization on the Dirichlet boundary, and we prove $O(h^2)$ convergence for the drag error. The approach employed for the theoretical study of the drag error uses duality arguments. Numerical tests illustrating the theoretical results are presented. The extension to other finite element methods is also discussed.

Keywords: Navier-Stokes, drag, convergence order, duality, stabilized finite elements, Nitsche's method

1. Introduction

We consider here an incompressible flow governed by the Navier-Stokes equations in a bounded domain of $\mathbb{R}^2$, approximated by a stabilized $(P_1)^2 \times P_1$ or $(Q_1)^2 \times Q_1$ continuous finite element method similar to the one introduced in [8]. We consider a Dirichlet condition on the inflow or the wall boundaries and a modified Neumann condition on the outflow (see [7]), allowing to treat re-entrant flows.

We recall that the drag on a closed and simply connected boundary Σ contained in the Dirichlet boundary is defined by

$$J(u) = \int_\Sigma (\mu \partial_n v - pn) \cdot e_1, \tag{1}$$

where $u = (v, p)$ with v the fluid's velocity and p its pressure, and e_1 is a given unit vector. In the case of a flow around an obstacle, e_1 is opposed to the obstacle's relative velocity.

In this paper, we are interested in defining a numerical drag value for which we can establish an improved convergence rate, under standard regularity assumptions. The proposed formula results from the weak formulation and takes into account the contribution of Nitsche's term on Σ, as well as a correction term related to the convection. A similar study can be carried out for the lift, replacing e_1 by an orthonormal vector e_2 in (1).

A direct bound of $|J(u_h) - J(u)|$ yields the same convergence order as $u - u_h$ in the $H^1(\Omega)^2 \times L^2(\Omega)$-norm, that is $O(h)$. However, it is known that the post-processing of certain quantities of physical interest such as displacements, stresses etc. can be computed with an improved convergence order. This was established in [1] for some model problems, by means of a duality argument. As regards the drag computation, this phenomenon was observed numerically for different finite element methods, see for instance [21], and more recently for B-splines/NURBS approximations in the framework of isogeometric analysis (see [18], [19]).

*corresponding author
Email address: daniela.capatina@univ-pau.fr (Daniela Capatina)

In the present work, we prove theoretically that the proposed numerical drag converges as $O(h^2)$ for the considered stabilized scheme. For this purpose, we use a duality technique as in optimization and control theory, or in goal-oriented a posteriori error estimates [9], [6].

As regards the numerical method, we consider here low-order continuous finite elements which need to be stabilized. Different weak formulations and stabilization forms exist in the literature. We have chosen the numerical approach proposed in [7], which presents several advantages: it enhances the coercivity of the discrete problem and yields an energy estimate, it allows to treat different types of boundary conditions in a unified manner, and it can also be applied in the limit case of the Euler equations. Note that the weak formulation contains antisymmetric terms related to the convection and the pressure.

We consider as interior stabilization the SUPG method proposed in [8], which follows the ideas of [13], [20]. We also stabilize both the Dirichlet and Neumann boundary conditions by means of a Nitsche's type method, similarly to [7]. We recall that Nitsche's method was originally developed to handle Dirichlet boundary conditions for elliptic problems [24], and then it has been extended to the Stokes and Navier-Stokes equations, see for instance [5], [15], [3]. The stabilization parameters in the SUPG and the boundary stabilization forms are chosen such that the scaling of the equations is preserved and that the method is robust with respect to the value of the viscosity.

In order to illustrate our approach, we first consider in Section 2 the Stokes equations discretized by continuous $(P_1)^2 \times P_1$ or $(Q_1)^2 \times Q_1$ finite elements with SUPG stabilization. In this linear case, the discrete drag contains one additional Nitsche's term and is defined as follows:

$$J^{\mathrm{S}}(u_h) = J(u_h) - \sum_{S \subset \Sigma} \int_S \frac{\gamma_1 \mu}{|S|} (v_h - v^D) \cdot e_1,$$

with v^D the Dirichlet data and $\gamma_1 > 0$ a stabilization parameter. We show $O(h^2)$ convergence rate for the drag error $J^S(u_h) - J(u)$.

We focus in Section 3 on the incompressible Navier-Stokes equations. Independently of the stabilization, the non-linearity of the problem leads to additional terms in the drag error. We show that all of them behave as $O(h^2)$, except for a certain boundary integral on Σ, which we add to the discrete drag. This leads us to define:

$$\tilde{J}^{\mathrm{NS}}(u_h) = J^{\mathrm{S}}(u_h) - \int_\Sigma \frac{\rho}{2} (v_{n,h} - v_n^D) v^D \cdot e_1 + \rho (v_n^D)^+ (v_h - v^D) \cdot e_1,$$

where v^D is the Dirichlet data on Σ.

Then we treat the stabilization terms. Similarly to the Stokes equations, we first consider in subsection 3.1 the discrete formulation with the interior stabilization proposed in [8]. We show that the contribution of the SUPG term to the drag error is of the same order as in the Stokes case, that is $O(h^2)$.

Next we study in subsection 3.2 the influence of the boundary stabilization terms. It turns out that the form living on the Neumann boundary introduced in [7] does not allow to improve the convergence rate for the drag error. Therefore, we propose here a modified stabilization which uses an adjoint boundary operator as well as a slightly different stabilization parameter. This new form preserves the good properties of the numerical scheme, in particular the consistency and the coercivity, and it yields a $O(h^2)$ drag error, with the new expression of the drag given below:

$$J^{\mathrm{NS}}(u_h) = \tilde{J}^{\mathrm{NS}}(u_h) - \int_\Sigma \theta_h^D (v_{n,h} - v_n^D) n \cdot e_1.$$

The additional term results from Nitsche's stabilization, similarly to the Stokes case, and θ_h^D is a stabilization parameter.

We present in Section 4 some numerical tests which illustrate the theoretical results, for both Stokes and Navier-Stokes systems. We first consider a manufactured solution, and then the well-known cylinder benchmark of [26] for which a reference drag value is known. We retrieve the expected convergence rate for the drag. We also present some numerical results for a time-dependent flow studied in the cylinder benchmark, and show that they compare well with the literature [22], [18].

Finally, let us note that the approach developed for the continuous $(P_1)^2 \times P_1$ and $(Q_1)^2 \times Q_1$ stabilized formulations can be applied to other finite element methods. In the appendices, we discuss two well-known approximations of the Navier-Stokes equations, both inf-sup stable: the conforming $(P_2)^2 \times P_1$ and the nonconforming $(P_1)^2 \times P_0$ methods. We show an improved convergence rate of the drag error for both discretizations.

2. Stokes equations

For the sake of simplicity, we assume in the theoretical analysis that Ω is a bounded polygonal domain of $\mathbb{R}^2$ and Γ^D, Γ^N a partition of its boundary. However, in the numerical tests we also treat the case of a curved boundary Σ, which is approximated by piece-wise second order polynomials (see for instance the cylinder benchmark). We denote by n the unit outward normal to $\partial\Omega$ and we assume that $\Gamma^D \neq \emptyset$.

We consider here the model problem:

$$\left\{\begin{array}{rll} -\mu\Delta v + \nabla p &= f & \text{in } \Omega \\ \text{div} v &= 0 & \text{in } \Omega \\ v &= v^D & \text{on } \Gamma^D \\ \mu\partial_n v - pn &= -p^N n & \text{on } \Gamma^N \end{array}\right. , \tag{2}$$

with data $f \in L^2(\Omega)^2$, $v^D \in H^{1/2}(\Gamma^D)^2$ and $p^N \in L^2(\Gamma^N)$.

The classical velocity-pressure variational formulation of (2) is given by:

$$u = (v,p) \in V^{v^D} \times L^2(\Omega), \qquad a^{\mathrm{S}}(u,\psi) = l^{\mathrm{S}}(\psi), \quad \forall \psi = (\phi,\chi) \in V^0 \times L^2(\Omega)$$

where

$$V^{v^D} = \left\{ v \in H^1(\Omega)^2;\ v_{|\Gamma^D} = v^D \right\}, \qquad V^0 = \left\{ v \in H^1(\Omega)^2;\ v_{|\Gamma^D} = 0 \right\},$$
$$a^{\mathrm{S}}(u,\psi) = \int_\Omega \mu\nabla v : \nabla\phi + \int_\Omega \chi \text{div} v - p\text{div}\phi, \qquad l^{\mathrm{S}}(\psi) = \int_\Omega f\cdot\phi - \int_{\Gamma^N} p^N \phi\cdot n.$$

We are interested in the computation of the drag $J(u)$ defined in (1), with $\Sigma \subset \Gamma^D$.

Let $\xi \in H^1(\Omega)^2$ any function satisfying $\xi = e_1$ on Σ and $\xi = 0$ on $\Gamma^D \setminus \Sigma$. We have, by using the continuous Stokes problem, that

$$J(u) = a^{\mathrm{S}}(u,\psi) - l^{\mathrm{S}}(\psi), \qquad \forall \psi \in V^\xi \times L^2(\Omega). \tag{3}$$

It is useful to consider the adjoint problem:

$$z = (z_v, z_p) \in V^\xi \times L^2(\Omega), \qquad a^{\mathrm{S}}(\eta, z) = 0, \quad \forall \eta = (\eta_v, \eta_p) \in V^0 \times L^2(\Omega).$$

It yields that:

$$\left\{\begin{array}{rll} \mu\Delta z_v + \nabla z_p &= 0 & \text{in } \Omega \\ \text{div} z_v &= 0 & \text{in } \Omega \\ z_v &= \xi & \text{on } \Gamma^D \\ \mu\partial_n z_v + z_p n &= 0 & \text{on } \Gamma^N \end{array}\right. .$$

For the finite element approximation of the Stokes equations, we consider either triangular or quadrilateral meshes. Let $(\mathcal{K}_h)_h$ be a regular family of meshes of Ω, $\bar{\Omega} = \cup_{K\in\mathcal{K}_h} K$; this ensures that the aspect ratio of the cells $K \in \mathcal{K}_h$ is uniformly bounded. Let $\mathcal{S}_h^{int}$ and $\mathcal{S}_h^D$ denote the set of interior and of Dirichlet sides, respectively.

We consider here the finite dimensional spaces of Lagrange finite elements of degree 1 for both the velocity and the pressure, denoted by V_h and M_h respectively. Let us recall that on a triangular mesh, one has

$$M_h = \left\{ \chi_h \in \mathcal{C}^0(\bar{\Omega});\ (\chi_h)_{|K} \in P_1, \quad \forall K \in \mathcal{K}_h \right\}, \qquad V_h = M_h^2.$$

On a quadrilateral mesh, one imposes in the definition of M_h that $(\chi_h \circ F_K)_{|\hat{K}} \in Q_1$, with $\hat{K}$ the reference element and $F_K : \hat{K} \to K$ the usual transformation.

We have chosen to treat the Dirichlet boundary condition by means of Nitsche's method. We begin by considering the following discrete formulation : $u_h = (v_h, p_h) \in V_h \times M_h$,

$$a^{\mathrm{S}}(u_h, \psi_h) - I_1(u_h, \phi_h) - I_2(\psi_h, v_h - v^D) + s(v_h - v^D, \phi_h) = l^{\mathrm{S}}(\psi_h), \quad \forall \psi_h = (\phi_h, \chi_h) \in V_h \times M_h$$

where:

$$I_1(u, \phi) = \int_{\Gamma^D} (\mu \partial_n v - pn) \cdot \phi, \quad I_2(\psi, v) = \int_{\Gamma^D} (\mu \partial_n \phi + \chi n) \cdot v, \quad s(v, \phi) = \sum_{S \in \mathcal{S}_h^D} \frac{\gamma_1 \mu}{|S|} \int_S v \cdot \phi.$$

This formulation is symmetric with respect to v and anti-symmetric with respect to p. Here above, $\gamma_1 > 0$ is a stabilization parameter, which can be chosen independently of the discretization parameter, see for instance [5],[15], [3].

Since the pair (V_h, M_h) is not inf-sup stable, the approximation method needs additional stabilization. We employ the well-known SUPG stabilization for the Stokes equations:

$$a^{\mathrm{S}}_{\mathrm{stab}}(u_h, \psi_h) = \sum_{K \in \mathcal{K}_h} d_K \int_K \frac{1}{\theta_S} (R(u_h) - f) \cdot R(\psi_h) + \sum_{K \in \mathcal{K}_h} \gamma_2 d_K \int_K \theta_S \mathrm{div} v_h \, \mathrm{div} \phi_h,$$

with

$$(\theta_S)_{|K} = \gamma_3 \frac{\mu}{d_K}, \qquad R(\psi_h) = -\mu \Delta \phi_h + \nabla \chi_h.$$

Note that since ϕ_h is a harmonic function on any cell K, we have $R(\psi_h) = \nabla \chi_h$ for any discrete test-function $\psi_h = (\phi_h, \chi_h)$. The stabilization parameters $\gamma_2 > 0$, $\gamma_3 > 0$ are numerical constants, while d_K denotes the diameter of the cell K.

We next add $a^{\mathrm{S}}_{\mathrm{stab}}(u_h, \psi_h)$ to the previously introduced bilinear form of the discrete problem. Clearly, the added term is consistent: $a^{\mathrm{S}}_{\mathrm{stab}}(u, \psi) = 0$ for any sufficiently smooth test-function ψ, since $R(u) - f = 0$ and $\mathrm{div} v = 0$.

So the discrete problem finally reads: $u_h = (v_h, p_h) \in V_h \times M_h$,

$$\begin{aligned} (a^{\mathrm{S}} + a^{\mathrm{S}}_{\mathrm{stab}})(u_h, \psi_h) - I_1(u_h, \phi_h) - I_2(\psi_h, v_h - v^D) + s(v_h - v^D, \phi_h) \\ = l^{\mathrm{S}}(\psi_h), \quad \forall \psi_h = (\phi_h, \chi_h) \in V_h \times M_h. \end{aligned} \tag{4}$$

For γ_1 large enough, the discrete problem is well-posed and yields an optimal $O(h)$ convergence rate for a smooth exact solution. More precisely, by putting for $\psi = (\phi, \chi)$:

$$\|\psi\|^2 = \mu |\phi|^2_{1,\Omega} + \frac{1}{\mu} \|\chi\|^2_{0,\Omega}, \quad |||\psi|||^2 = \|\psi\|^2 + \sum_{S \in \mathcal{S}_h^D} \frac{\gamma_1 \mu}{|S|} \|\phi\|^2_{0,S},$$

we have for $u = (v, p) \in H^2(\Omega)^2 \times H^1(\Omega)$:

$$|||u - u_h|||^2 + a^{\mathrm{S}}_{\mathrm{stab}}(u - u_h, u - u_h) \leq c h^2.$$

In the following, we are interested in defining a discrete drag value and in establishing an improved convergence rate of the drag error for the approximation method (4), under the regularity assumptions u, $z \in H^2(\Omega)^2 \times H^1(\Omega)$.

Let us note that $J(u) = I_1(u, \xi)$. Then we define the discrete counterpart of the drag by:

$$J^{\mathrm{S}}(u_h) = I_1(u_h, \xi) - s(v_h - v^D, \xi) = \sum_{S \subset \Sigma} \int_S \left(\mu \partial_n v_h - p_h n - \frac{\gamma_1 \mu}{|S|} (v_h - v^D) \right) \cdot e_1.$$

It is useful to introduce an interpolation $\mathcal{L}_h z$ of z in $V_h \times M_h$, satisfying $\mathcal{L}_h z_v = \xi$ on Γ^D.

Remark 1. *One can employ the Lagrange interpolation operator for $z_v \in C^0(\bar{\Omega})$; it clearly satisfies the boundary condition $\mathcal{L}_h z_v = z_v$ on Γ^D. As regards the pressure z_p, which may be discontinuous, one can interpolate it by means of a Clément type operator.*

Lemma 1. *One has that*

$$J^{\mathrm{S}}(u_h) - J(u) = \mathcal{T}^{\mathrm{S}} + a^{\mathrm{S}}_{\mathrm{stab}}(u_h, \mathcal{L}_h z), \tag{5}$$

where

$$\mathcal{T}^{\mathrm{S}} = a^{\mathrm{S}}(u_h - u, \mathcal{L}_h z - z) - I_2(\mathcal{L}_h z - z, v_h - v). \tag{6}$$

Proof. By definition of J^{S} and J, we have:

$$J^{\mathrm{S}}(u_h) - J(u) = I_1(u_h - u, \xi) - s(v_h - v^D, \xi).$$

We next take $\xi = \mathcal{L}_h z_v$, which belongs to both V_h and $H^1(\Omega)^2$. So, we get thanks to the discrete problem (4) and to (3) with the test-function $\mathcal{L}_h z$ that:

$$J^{\mathrm{S}}(u_h) - J(u) = a^{\mathrm{S}}(u_h - u, \mathcal{L}_h z) - I_2(\mathcal{L}_h z, v_h - v^D) + a^{\mathrm{S}}_{\mathrm{stab}}(u_h, \mathcal{L}_h z).$$

By means of an integration by parts and of the adjoint boundary value problem, we also have that:

$$a^{\mathrm{S}}(\eta, z) = I_2(z, \eta_v), \quad \forall \eta = (\eta_v, \eta_p) \in H^1(\Omega)^2 \times L^2(\Omega). \tag{7}$$

So by using (7) with the test-function $u_h - u$, we obtain

$$\begin{aligned} J^{\mathrm{S}}(u_h) - J(u) &= a^{\mathrm{S}}(u_h - u, \mathcal{L}_h z - z) + I_2(z, v_h - v) - I_2(\mathcal{L}_h z, v_h - v^D) + a^{\mathrm{S}}_{\mathrm{stab}}(u_h, \mathcal{L}_h z) \\ &= \mathcal{T}^{\mathrm{S}} + a^{\mathrm{S}}_{\mathrm{stab}}(u_h, \mathcal{L}_h z). \end{aligned}$$

□

Theorem 1. *Under the regularity assumptions u, $z \in H^2(\Omega)^2 \times H^1(\Omega)$, one has that*

$$|J(u) - J^{\mathrm{S}}(u_h)| \leq ch^2.$$

Proof. The Cauchy-Schwarz inequality applied to (5) yields, for $\gamma_1 \geq 1$, that:

$$\begin{aligned} |J(u) - J^{\mathrm{S}}(u_h)| \leq & |||u - u_h||| \left(\|z - \mathcal{L}_h z\|^2 + \sum_{S \in \mathcal{S}_h^D} |S| (\mu \, \|\partial_n (z_v - \mathcal{L}_h z_v)\|^2_{0,S} + \frac{1}{\mu} \, \|z_p - \mathcal{L}_h z_p\|^2_{0,S}) \right)^{1/2} \\ & + |a^{\mathrm{S}}_{\mathrm{stab}}(u_h, \mathcal{L}_h z)|. \end{aligned}$$

We next use the approximation error estimate for $|||u - u_h|||$, the interpolation error estimate for $\|z - \mathcal{L}_h z\|$ as well as the following trace inequalities on $S \in \mathcal{S}_h^D \cap \partial K$:

$$|S|^{1/2} \, \|\partial_n (z_v - \mathcal{L}_h z_v)\|_{0,S} \leq c|S| \left(d_K^{-1} |z_v - \mathcal{L}_h z_v|_{1,K} + |z_v - \mathcal{L}_h z_v|_{2,K} \right) \leq c d_K |z_v|_{2,K},$$

$$|S|^{1/2} \, \|z_p - \mathcal{L}_h z_p\|_{0,S} \leq c|S| \left(d_K^{-1} \|z_p - \mathcal{L}_h z_p\|_{0,K} + |z_p - \mathcal{L}_h z_p|_{1,K} \right) \leq c d_K |z_p|_{1,\omega_K}.$$

Using that $\mathrm{div} v = \mathrm{div} z_v = 0$ and that $R(u_h - u)$, $R(\mathcal{L}_h z)$ are uniformly bounded in $L^2(K)^2$ for any $K \in \mathcal{K}_h$, we next obtain:

$$a^{\mathrm{S}}_{\mathrm{stab}}(u_h, \mathcal{L}_h z) = \sum_{K \in \mathcal{K}_h} \frac{d_K^2}{\gamma_3 \mu} \int_K R(u_h - u) \cdot R(\mathcal{L}_h z) + \sum_{K \in \mathcal{K}_h} \gamma_2 \gamma_3 \mu \int_K \mathrm{div}(v - v_h) \mathrm{div}(z_v - \mathcal{L}_h z_v)$$

which yields, by bounding the L^2-norm of the divergence by the H^1 semi-norm, that

$$|a^{\mathrm{S}}_{\mathrm{stab}}(u_h, \mathcal{L}_h z)| \leq ch^2.$$

We can thus deduce the announced estimate. □

3. Navier-Stokes equations

We now consider the steady, incompressible Navier-Stokes equations:

$$\begin{cases} \rho v \cdot \nabla v - \mu \Delta v + \nabla p &= f \qquad \text{in } \Omega \\ \qquad\qquad\qquad \text{div} v &= 0 \qquad \text{in } \Omega, \end{cases} \tag{8}$$

satisfying the same Dirichlet boundary conditions as in (2), but a modified outflow condition allowing for a better treatment of re-entrant flows (cf. [7]):

$$\rho v_n^- v - \mu \partial_n v + pn = p^N n \qquad \text{on } \Gamma^N, \tag{9}$$

where a^- stands for the negative part of a and is defined by $a^- = (a - |a|)/2$.

The solution of the continuous problem satisfies the weak formulation: $u = (v, p) \in V^{v^D} \times L^2(\Omega)$,

$$a^{\text{NS}}(u)(\psi) = l^{\text{NS}}(u)(\psi), \quad \forall \psi = (\phi, \chi) \in V^0 \times L^2(\Omega),$$

where:

$$a^{\text{NS}}(u)(\psi) = a^{\text{S}}(u, \psi) + a^{\text{c}}(u)(\psi), \qquad l^{\text{NS}}(u)(\psi) = l^{\text{S}}(\psi) + l^{\text{c}}(u)(\psi)$$

and

$$\begin{aligned} a^{\text{c}}(u)(\psi) &= \int_\Omega \frac{\rho}{2} \left((v \cdot \nabla v) \cdot \phi - v \cdot (v \cdot \nabla \phi) \right) + \int_{\partial\Omega} \frac{\rho}{2} |v_n| v \cdot \phi, \\ l^{\text{c}}(u)(\psi) &= - \int_{\Gamma^D} \rho v_n^- v^D \cdot \phi. \end{aligned}$$

By using the continuous problem, we now have for the drag that

$$J(u) = I_1(u, \xi) = a^{\text{NS}}(u)(\psi) - l^{\text{NS}}(u)(\psi), \qquad \forall \psi = (\xi, \chi) \in V^\xi \times L^2(\Omega). \tag{10}$$

We next introduce the adjoint problem: $z = (z_v, z_p) \in V^\xi \times L^2(\Omega)$,

$$(a^{\text{NS}})'_u(\eta, z) = 0, \quad \forall \eta = (\eta_v, \eta_p) \in V^0 \times L^2(\Omega). \tag{11}$$

The bilinear form $(a^{\text{NS}})'_u$ is defined as follows:

$$\begin{aligned} (a^{\text{NS}})'_u(\eta, z) =& a^{\text{S}}(\eta, z) + \int_\Omega \frac{\rho}{2} \left((v \cdot \nabla \eta_v + \eta_v \cdot \nabla v) \cdot z_v - v \cdot (\eta_v \cdot \nabla z_v) - \eta_v \cdot (v \cdot \nabla z_v) \right) \\ &+ \int_{\partial\Omega} \frac{\rho}{2} \left(\text{sgn}(v_n) \eta_{v,n} v + |v_n| \, \eta_v \right) \cdot z_v, \end{aligned}$$

where we have used that $(x\,|x|)' = \text{sgn}(x)x + |x|$. Thus, the adjoint problem yields the following equations

$$-\rho v \cdot \nabla z_v + \frac{\rho}{2} (\nabla v)^T z_v - \frac{\rho}{2} (\nabla z_v)^T v - \mu \triangle z_v - \nabla z_p = 0, \qquad \text{div} z_v = 0 \quad \text{in } \Omega. \tag{12}$$

In order to retrieve the boundary condition on Γ^N, we integrate by parts in (11) and we obtain:

$$\int_{\Gamma^N} \left(\mu \partial_n z_v + z_p n + \frac{\rho}{2} (v_n + |v_n|) z_v + \frac{\rho}{2} \text{sgn}(v_n)(v \cdot z_v) n \right) \cdot \eta_v = 0, \qquad \forall \eta_v \in V^0.$$

We further use the relation $x + |x| = 2x^+$ and get

$$\rho v_n^+ z_v + \frac{\rho}{2} \text{sgn}(v_n)(v \cdot z_v) n + \mu \partial_n z_v + z_p n = 0 \qquad \text{on } \Gamma^N. \tag{13}$$

This finally yields, for any $\eta = (\eta_v, \eta_p) \in H^1(\Omega)^2 \times L^2(\Omega)$, that

$$(a^{\rm NS})'_u(\eta, z) = I_2(z, \eta_v) + \int_{\Gamma^D} \left(\rho v_n^+ z_v + \frac{\rho}{2} {\rm sgn}(v_n)(v \cdot z_v) n \right) \cdot \eta_v. \tag{14}$$

For simplicity of the writing, it is useful to introduce the operators associated with the boundary conditions on Γ^N for the direct and the adjoint problems:

$$\begin{aligned} \mathcal{C}(u) =& \rho v_n^- v_n - \mu \partial_n v \cdot n + p, \\ \mathcal{C}^{\rm adj}(u)(\psi) =& \rho v_n^+ \phi_n + \frac{\rho}{2} {\rm sgn}(v_n) v \cdot \phi + \mu \partial_n \phi \cdot n + \chi. \end{aligned}$$

Considering the normal component in (9) and (13) yields $\mathcal{C}(u) = p^N$ and $\mathcal{C}^{\rm adj}(u)(z) = 0$.

We employ the same pairs of discrete spaces (V_h, M_h) as for the Stokes equations, that is P_1 or Q_1 continuous elements for both the velocity and the pressure. We add two types of stabilization: a interior SUPG one, denoted by $a^{\rm NS}_{\rm stab}$, as well as a boundary stabilization of Nitsche's type, denoted by s^{∂}.

In order to establish an improved convergence rate for the drag error, the discrete drag needs to be corrected by additional terms.

3.1. Drag correction due to SUPG stabilization

We consider the following consistent form, proposed and studied in [8]:

$$a^{\rm NS}_{\rm stab}(u)(\psi) = \sum_{K \in \mathcal{K}_h} d_K \int_K \frac{1}{\theta} (R_u(u) - f) \cdot R_u(\psi) + \sum_{K \in \mathcal{K}_h} \gamma_2 d_K \int_K \theta {\rm div} v {\rm div} \phi,$$

where

$$R_u(\psi) = \rho v \cdot \nabla \phi - \mu \Delta \phi + \nabla \chi.$$

The role of the parameter $\theta = \theta(v)$ is to balance this additional term such that it has the same scaling as $a^{\rm NS}$. It may depend on the solution itself, on the physical parameters as well as on the discretization parameters. The choice of [8] is to take, in the steady case,

$$\theta^2(v_h)_{|K} = \gamma_3^2 \left(\frac{\mu}{d_K} \right)^2 + \gamma_4^2 |\rho v_h|^2, \qquad \forall K \in \mathcal{K}_h, \tag{15}$$

where the additional parameter $\gamma_4 > 0$ is a numerical constant. In the sequel, we shall denote $\theta(v_h)$ by θ_h. Note that it is not constant on $K \in \mathcal{K}_h$.

Remark 2. *This choice is clearly compatible with the Stokes case, for which $\gamma_4 = 0$ and $\theta = \theta_S$. Thus, $a^{\rm NS}_{\rm stab}$ clearly extends $a^{\rm S}_{\rm stab}$ to the Navier-Stokes case. Also note that in the case of vanishing velocity, the stabilization parameters of $a^{\rm NS}_{\rm stab}$ are similar to those used for the Brinkman equation cf. [2], [12].*

Remark 3. *For the first term of $a^{\rm NS}_{\rm stab}$, we have a similar expression of the stabilization parameter to the one of [17]. For the second term, we recover a similar parameter to [17] in the case of large Péclet numbers, whereas in the case of small Péclet numbers, it corresponds to the Stokes stabilization parameter.*

This leads us to consider the following discrete formulation of the Navier-Stokes equations: $u_h = (v_h, p_h) \in V_h \times M_h$,

$$\begin{aligned} (a^{\rm NS} + a^{\rm NS}_{\rm stab})(u_h)(\psi_h) - I_1(u_h, \phi_h) - I_2(\psi_h, v_h - v^D) + s(v_h - v^D, \phi_h) \\ = l^{\rm NS}(u_h)(\psi_h), \qquad \forall \psi_h = (\phi_h, \chi_h) \in V_h \times M_h. \end{aligned} \tag{16}$$

As for the Stokes problem, we assume that for $u \in H^2(\Omega)^2 \times H^1(\Omega)$ and for γ_1 sufficiently large, we have:

$$|||u - u_h||| \leq ch. \tag{17}$$

By equivalence of the $H^1(\Omega)$-norm and the energy norm $|||\cdot|||$ on V_h, together with a triangular inequality, it follows that

$$\|v - v_h\|_{0,\Omega} \leq ch.$$

In addition, we assume that

$$\|u - u_h\|_{0,\Omega} \leq ch^2, \tag{18}$$

which is usually proved by means of an Aubin-Nitsche duality argument. The convergence rates (17) and (18) were checked numerically in [7].

We are next interested in estimating the drag error, under the regularity assumption:

$$z \in H^2(\Omega)^2 \times H^1(\Omega). \tag{19}$$

Remark 4. *This assumption may not be checked for certain configurations, in particular when $\overline{\Sigma}$ and $\overline{\Gamma^D \setminus \Sigma}$ are not disjoint. However, we can carry on exactly the same analysis under a weaker assumption $z \in H^{1+l}(\Omega)^2 \times H^l(\Omega)$ and prove an $O(h^{1+l})$ convergence rate for the drag error.*

As regards the discrete value of the drag, let us begin by considering the same expression as in the Stokes case and by evaluating the error $J^{\mathrm{S}}(u_h) - J(u)$. We obviously have, thanks to the relation $\mathcal{L}_h z_v = \xi$ on Γ^D, that

$$J^{\mathrm{S}}(u_h) - J(u) = I_1(u_h - u, \mathcal{L}_h z_v) - s(v_h - v^D, \mathcal{L}_h z_v).$$

By using (10) with the test-function $\mathcal{L}_h z \in V^\xi \times L^2(\Omega)$, as well as the discrete problem (16), we get

$$\begin{aligned} J^{\mathrm{S}}(u_h) - J(u) =& a^{\mathrm{NS}}(u_h)(\mathcal{L}_h z) - a^{\mathrm{NS}}(u)(\mathcal{L}_h z) - I_2(\mathcal{L}_h z, v_h - v) \\ &+ l^{\mathrm{NS}}(u)(\mathcal{L}_h z) - l^{\mathrm{NS}}(u_h)(\mathcal{L}_h z) + a^{\mathrm{NS}}_{\mathrm{stab}}(u_h)(\mathcal{L}_h z) \\ =& \mathcal{T}^{\mathrm{S}} + \mathcal{T}^{\mathrm{c}} + \mathcal{T}^{\mathrm{lin}} + \mathcal{T}^{\mathrm{rhs}} + \mathcal{T}^{\mathrm{adj}} + \mathcal{T}^{\mathrm{stab}}, \end{aligned}$$

where $\mathcal{T}^{\mathrm{S}}$ is defined in (6) and the other terms take into account different aspects related to the non-linearity and the stabilization of the Navier-Stokes equations. They are defined as follows:

$$\begin{aligned} \mathcal{T}^{\mathrm{c}} =& a^{\mathrm{c}}(u_h)(\mathcal{L}_h z - z) - a^{\mathrm{c}}(u)(\mathcal{L}_h z - z), \\ \mathcal{T}^{\mathrm{lin}} =& a^{\mathrm{c}}(u_h)(z) - a^{\mathrm{c}}(u)(z) - (a^{\mathrm{c}})'_u(u_h - u, z), \\ \mathcal{T}^{\mathrm{rhs}} =& l^{\mathrm{c}}(u)(\mathcal{L}_h z) - l^{\mathrm{c}}(u_h)(\mathcal{L}_h z), \\ \mathcal{T}^{\mathrm{adj}} =& (a^{\mathrm{NS}})'_u(u_h - u, z) - I_2(z, v_h - v), \\ \mathcal{T}^{\mathrm{stab}} =& a^{\mathrm{NS}}_{\mathrm{stab}}(u_h)(\mathcal{L}_h z). \end{aligned}$$

The terms $\mathcal{T}^{\mathrm{c}}$ and $\mathcal{T}^{\mathrm{lin}}$ take into account the non-linearity of the convective term in the form a^{c}.

Since $\mathcal{L}_h z_v = z_v$ on Γ^D, $\mathcal{T}^{\mathrm{c}}$ can be written as follows:

$$\begin{aligned} \mathcal{T}^{\mathrm{c}} =& \int_\Omega \frac{\rho}{2}((v_h - v)\cdot\nabla v_h + v\cdot\nabla(v_h - v))\cdot(\mathcal{L}_h z_v - z_v) \\ &- \int_\Omega \frac{\rho}{2}(v_h - v)\cdot(v_h\cdot\nabla(\mathcal{L}_h z_v - z_v)) + \frac{\rho}{2} v\cdot((v_h - v)\cdot\nabla(\mathcal{L}_h z_v - z_v)) \\ &+ \int_{\Gamma^N} \frac{\rho}{2}(|v_{n,h}|(v_h - v) + (|v_{n,h}| - |v_n|)v)\cdot(\mathcal{L}_h z_v - z_v) \end{aligned}$$

and is of second order $O(h^2)$, like $\mathcal{T}^{\mathrm{S}}$.

As regards $\mathcal{T}^{\rm lin}$, let us compute separately the contributions on Ω and on $\partial\Omega$, respectively. The contribution on Ω is given by:

$$\begin{aligned}\mathcal{T}^{\rm lin,\Omega} &= \int_\Omega \frac{\rho}{2}\left((v_h\cdot\nabla v_h)\cdot z_v - v_h\cdot(v_h\cdot\nabla z_v) - (v\cdot\nabla v)\cdot z_v + v\cdot(v\cdot\nabla z_v)\right)\\ &\quad - \int_\Omega \frac{\rho}{2}\left((v\cdot\nabla(v_h-v)+(v_h-v)\cdot\nabla v)\cdot z_v - v\cdot(v_h-v)\cdot\nabla z_v - (v_h-v)\cdot(v\cdot\nabla z_v)\right)\\ &= \int_\Omega \frac{\rho}{2}\Big((v_h-v)\cdot\nabla(v_h-v)\cdot z_v - (v_h-v)\cdot((v_h-v)\cdot\nabla z_v)\Big)\end{aligned}$$

and is also of second order. Meanwhile, the contribution on $\partial\Omega$ is given by:

$$\mathcal{T}^{\rm lin,\partial\Omega} = \int_{\partial\Omega}\frac{\rho}{2}(|v_{n,h}|v_h\cdot z_v - |v_n|v\cdot z_v) - \int_{\partial\Omega}\frac{\rho}{2}(\mathrm{sgn}(v_n)(v_{n,h}-v_n)v\cdot z_v + |v_n|\,(v_h-v)\cdot z_v).$$

On $\Gamma^D\setminus\Sigma$ we have $z_v=0$ whereas on Σ we have $z_v=e_1$, such that:

$$\begin{aligned}\mathcal{T}^{\rm lin,\partial\Omega} &= \int_\Sigma\frac{\rho}{2}(|v_{n,h}|-|v_n|)v_h\cdot e_1 - \int_\Sigma\frac{\rho}{2}\mathrm{sgn}(v_n)(v_{n,h}-v_n)v\cdot e_1\\ &\quad + \int_{\Gamma^N}\frac{\rho}{2}(|v_{n,h}|-|v_n|)v_h\cdot z_v - \int_{\Gamma^N}\frac{\rho}{2}\mathrm{sgn}(v_n)(v_{n,h}-v_n)v\cdot z_v\\ &= \int_{\partial\Omega}\frac{\rho}{2}(|v_{n,h}|-|v_n|)(v_h-v)\cdot z_v + \int_{\Gamma^N}\frac{\rho}{2}\left(\mathrm{sgn}(v_{n,h})-\mathrm{sgn}(v_n)\right)v_{n,h}v\cdot z_v\\ &\quad + \int_\Sigma\frac{\rho}{2}\left(|v_{n,h}|-|v_n^D| - \mathrm{sgn}(v_n^D)(v_{n,h}-v_n^D)\right)v^D\cdot e_1.\end{aligned}$$

$\mathcal{T}^{\rm rhs}$ reflects the non-linearity of the right-hand side term and can be written as follows:

$$\mathcal{T}^{\rm rhs} = \int_\Sigma \rho\left(v_{n,h}^- - (v_n^D)^-\right)v^D\cdot e_1.$$

$\mathcal{T}^{\rm adj}$ corresponds to (7) in the Stokes case, where it was null; by using (14) with the test-function $u_h-u\in H^1(\Omega)^2\times L^2(\Omega)$, as well as the relation $z_v=\xi$ on Γ^D, we get

$$\mathcal{T}^{\rm adj} = \int_\Sigma \rho(v_n^D)^+(v_h-v^D)\cdot e_1 + \frac{\rho}{2}\mathrm{sgn}(v_n^D)(v_{n,h}-v_n^D)v^D\cdot e_1.$$

Finally, the following lemma shows that the remaining term $\mathcal{T}^{\rm stab}$ resulting from the stabilization is of higher order.

Lemma 2. *Under the assumptions (17) and (19), one has that*

$$|\mathcal{T}^{\rm stab}|\le c\,h^2.$$

Proof. We write that

$$\begin{aligned}a_{\rm stab}^{\rm NS}(u_h)(\mathcal{L}_h z) &= \sum_{K\in\mathcal{K}_h} d_K\int_K\frac{1}{\theta_h}(R_{u_h}(u_h)-f)\cdot R_{u_h}(\mathcal{L}_h z)\\ &\quad + \sum_{K\in\mathcal{K}_h}\gamma_2 d_K\int_K\theta_h\mathrm{div}(v_h-v)\mathrm{div}(\mathcal{L}_h z_v - z_v).\end{aligned}\tag{20}$$

Concerning the first sum of (20), we note that the choice (15) of θ_h ensures that

$$\frac{1}{|\theta_h|_{\infty,K}}\le\frac{d_K}{\gamma_3\mu},\qquad\forall K\in\mathcal{K}_h.$$

So by using that $R_{u_h}(u_h) - f$ and $R_{u_h}(\mathcal{L}_h z)$ are uniformly bounded in $L^2(K)^2$ for any $K \in \mathcal{K}_h$, we obtain the desired convergence rate $O(h^2)$. As regards the second sum of (20), we bound it thanks to the interpolation error, the approximation error and the following inequality:

$$|\theta_h|_{\infty,K} \leq \frac{1}{d_K}\left(\gamma_3\mu + \gamma_4 d_K |\rho v_h|_{\infty,K}\right) \leq \frac{1}{d_K}\left(\gamma_3\mu + c\gamma_4 \|\rho v_h\|_{0,K}\right) \leq \frac{c}{d_K}, \qquad \forall K \in \mathcal{K}_h.$$

Thus, it finally follows that

$$|a_{\text{stab}}^{\text{NS}}(u_h)(\mathcal{L}_h z)| \leq ch^2.$$

□

We can now sum up all the previous contributions and gather them in three terms:

$$J^{\text{S}}(u_h) - J(u) = \mathcal{T}^{\text{h.o.t.}} + \mathcal{T}^N + \mathcal{T}^\Sigma,$$

where $\mathcal{T}^{\text{h.o.t.}}$ contains all the higher order terms, $\mathcal{T}^N$ represents the remaining integral on Γ^N in $\mathcal{T}^{\text{lin},\partial\Omega}$ and $\mathcal{T}^\Sigma$ contains the integrals on Σ in $\mathcal{T}^{\text{lin},\partial\Omega}$, $\mathcal{T}^{\text{rhs}}$, $\mathcal{T}^{\text{adj}}$ which are of the same convergence order as the solution. We have that:

$$\begin{aligned}
\mathcal{T}^{\text{h.o.t.}} =& \mathcal{T}^{\text{S}} + \mathcal{T}^{\text{c}} + \mathcal{T}^{\text{lin},\Omega} + \mathcal{T}^{\text{stab}} + \int_{\partial\Omega} \frac{\rho}{2}(|v_{n,h}| - |v_n|)(v_h - v)\cdot z_v, \\
\mathcal{T}^N =& \int_{\Gamma^N} \frac{\rho}{2}\left(\text{sgn}(v_{n,h}) - \text{sgn}(v_n)\right) v_{n,h} v \cdot z_v, \\
\mathcal{T}^\Sigma =& \int_\Sigma \rho\left(v_{n,h}^- - (v_n^D)^-\right) v^D \cdot e_1 + \rho(v_n^D)^+(v_h - v^D)\cdot e_1 + \frac{\rho}{2}(|v_{n,h}| - |v_n^D|)v^D \cdot e_1 \\
=& \int_\Sigma \frac{\rho}{2}(v_{n,h} - v_n^D)v^D \cdot e_1 + \rho(v_n^D)^+(v_h - v^D)\cdot e_1.
\end{aligned} \tag{21}$$

In order to get a higher order convergence for the drag error, we propose to take as discrete drag value for the Navier-Stokes equations:

$$\tilde{J}^{\text{NS}}(u_h) = J^{\text{S}}(u_h) - \mathcal{T}^\Sigma \tag{22}$$

that is:

$$\tilde{J}^{\text{NS}}(u_h) = \sum_{S\subset\Sigma}\int_S \left(\mu\partial_n v_h - p_h n - \frac{\gamma_1\mu}{|S|}(v_h - v^D) - \rho(v_n^D)^+(v_h - v^D) - \frac{\rho}{2}(v_{n,h} - v_n^D)v^D\right)\cdot e_1.$$

Thus, we can write that:

$$\tilde{J}^{\text{NS}}(u_h) - J(u) = \mathcal{T}^{\text{h.o.t.}} + \mathcal{T}^N. \tag{23}$$

Thanks to Lemma 2, we have shown so far the following estimate:

$$|\mathcal{T}^{\text{h.o.t.}}| \leq ch^2. \tag{24}$$

Lemma 3. *Assume (17), (18) and (19). Then one has that*

$$|\mathcal{T}^N| \leq ch^2. \tag{25}$$

Proof. By using the relation $\text{sgn}(a)a = |a|$ as well as the triangle inequality, we can bound the next term as follows:

$$\begin{aligned}
|(\text{sgn}(v_{n,h}) - \text{sgn}(v_n))v_{n,h}| =& ||v_{n,h}| - |v_n| + \text{sgn}(v_n)(v_n - v_{n,h})| \\
\leq& |v_{n,h} - v_n| + |\text{sgn}(v_n)||v_n - v_{n,h}| \leq 2|v_n - v_{n,h}|.
\end{aligned}$$

Thus, we get that

$$|\mathcal{T}^N| \leq \int_{\Gamma^N} \rho|v_n - v_{n,h}||v\cdot z_v| \leq \|v_n - v_{n,h}\|_{L^1(\Gamma^N)}\|\rho v\cdot z_v\|_{L^\infty(\Gamma^N)}.$$

The regularity assumptions on v and z_v allow us to bound the last term, by using Sobolev's embedding theorem in Ω, leading thus to

$$|\mathcal{T}^N| \leq c \sum_{S \in \mathcal{S}_h^N} \|v - v_h\|_{L^1(S)}.$$

Thanks to the Cauchy-Schwarz inequality and to the trace theorem, we have for any side $S \subset \Gamma^N$ that

$$\|v - v_h\|_{L^1(S)} \leq |S|^{1/2} \|v - v_h\|_{0,S} \leq c(\|v - v_h\|_{0,K} + d_K |v - v_h|_{1,K}),$$

where $K \in \mathcal{K}_h$ is the cell containing the side S. Finally, by summing upon S and by using the assumption (18), we obtain the announced result:

$$|\mathcal{T}^N| \leq c(\|v - v_h\|_{0,\Omega} + h|v - v_h|_{1,\Omega}) \leq ch^2.$$

□

Remark 5. *If* $\mathrm{sgn}(v_n) = \mathrm{sgn}(v_{n,h})$ *on the outflow boundary* Γ^N*, then one has* $\mathcal{T}^N = 0$ *and assumption (18) is not necessary.*

Gathering together the estimates (24) and (25), we obtain from (23) the next result.

Theorem 2. *Under the regularity assumptions (17), (18) and (19), one has that:*

$$|\tilde{J}^{\mathrm{NS}}(u_h) - J(u)| \leq c\, h^2.$$

3.2. Drag correction due to Nitsche's formulation

In this section, we focus on the stabilization of the boundary conditions.

Let us note that without any stabilization, the energy norm does not contain any pressure term and degenerates for small values of the viscosity and of v_n on $\partial\Omega$. Indeed, if we denote by A the operator of the discrete Navier-Stokes problem without SUPG stabilization, then we have for any $\psi_h = (\phi_h, \chi_h) \in V_h \times M_h$ that

$$A(\psi_h)(\psi_h) \simeq \mu |\phi_h|^2_{1,\Omega} + \sum_{S \in \mathcal{S}_h^D} \frac{\mu}{|S|} \int_S \phi_h^2 + \int_{\partial\Omega} \frac{\rho}{2} |\phi_{n,h}| \phi_h^2. \tag{26}$$

In order to improve the robustness of the numerical scheme, we add, besides the previous SUPG stabilization, some stabilization on the boundary. The additional terms should also be consistent and have the same scaling as the main operator.

Such a stabilization was proposed in [7] for more general boundary conditions. It allows to treat a large range of viscosity values, including the limit case of the Euler equations, and to control the discrete kinetic energy in the unsteady case. It can be written as follows:

$$\int_{\Gamma^N} \frac{1}{\theta} (\mathcal{C}(u_h) - p^N) \mathcal{C}(\psi_h) + \int_{\Gamma^D} \theta (v_{n,h} - v_n^D) \phi_{n,h}. \tag{27}$$

It is shown in [7] that this leads to the additional term $\displaystyle\int_{\Gamma^N} \chi_h^2/\theta + \int_{\Gamma^D} \theta \phi_{h,n}^2$ in the energy norm. Modifications of the outflow condition aimed to increase stability in the case of re-entrant flows have also been proposed in [14], [4], [11] from a different point of view, but they do not allow to control the pressure and the normal velocity. A recent review on stabilizations of outflow boundary conditions can be found in [10].

The parameter θ scales as $\rho|v_n|$ and $\mu/|S|$. The choice of [7] for the steady case is

$$\theta^2 (v_h)_{|S} = \gamma_3^2 \frac{\mu^2}{|S|^2} + \gamma_4^2 (\rho v_{n,h})^2, \quad \forall S \in \mathcal{S}_h^\partial. \tag{28}$$

Note that (28) is compatible with the expression (15) of θ for the SUPG stabilization, with d_K and $|v_h|$ replaced by $|S|$ and $|v_{n,h}|$, respectively.

Unfortunately, the boundary stabilization (27) does not allow to establish an optimal convergence rate for the drag error. Indeed, we show below that the additional term in the drag error is the first integral of (27) with $\psi_h = \mathcal{L}_h z$, but then the resulting term $\mathcal{C}(\mathcal{L}_h z)$ cannot be controlled. This leads us to replace $\mathcal{C}(\psi_h)$ by $\mathcal{C}^{\rm adj}(u_h)(\psi_h)$, which will be bounded for $\psi_h = \mathcal{L}_h z$ by using that $\mathcal{C}^{\rm adj}(u)(z) = 0$. In order to preserve the coercivity with respect to the energy norm, we also have to modify the stabilization parameter on Γ^N.

Therefore, we propose here the following boundary stabilization:

$$s^{\partial}(u_h)(\psi_h) = \int_{\Gamma^N} \theta^N (\mathcal{C}(u_h) - p^N)\mathcal{C}^{\rm adj}(u_h)(\psi_h) + \int_{\Gamma^D} \theta^D (v_{n,h} - v_n^D)\phi_{n,h},$$

where on any side $S \in \mathcal{S}_h^N$ we define point-wise:

$$\left(\theta^N\right)^2(v_h) = \frac{v_{n,h}^2 |S|^2}{\gamma_3^2 \mu^2 v_{n,h}^2 + \gamma_4^2 |S|^2 (\rho v_h^2)^2} \ \text{ if } |v_h| \neq 0, \qquad \theta^N(v_h) = \frac{|S|}{\gamma_3 \mu} \ \text{ if } |v_h| = 0$$

and on any $S \in \mathcal{S}_h^D$ we take $\theta^D(v_h) = \theta(v_h)$ defined in (28). As previously, we denote $\theta^N(v_h)$ and $\theta^D(v_h)$ by θ_h^N and θ_h^D, respectively.

The new form s^{∂} has the same properties as the stabilization of [7]. It is clearly consistent and it respects the scaling, since both θ_h^N and θ_h^D scale as θ_h.

It is important to note that we have, on any side $S \in \mathcal{S}_h^N$,

$$\theta_h^N \leq \frac{|S|}{\gamma_3 \mu}, \tag{29}$$

as well as

$$\rho v_h^2 \theta_h^N \leq \frac{|v_{n,h}|}{\gamma_4}. \tag{30}$$

The first inequality is used in the proof of the convergence rate of the drag error (see Theorem 4), whereas the second inequality is crucial for the discrete coercivity (see Theorem 3).

Theorem 3. *Let $\psi_h = (\phi_h, \chi_h) \in V_h \times M_h$ and let $\theta_h^N = \theta^N(\phi_h)$, $\theta_h^D = \theta^D(\phi_h)$. Then for γ_1, γ_3 and γ_4 sufficiently large and for vanishing data, one has:*

$$\begin{aligned} A(\psi_h)(\psi_h) + a_{\rm stab}^{\rm NS}(\psi_h)(\psi_h) + s^{\partial}(\psi_h)(\psi_h) \gtrsim \mu |\phi_h|_{1,\Omega}^2 + \sum_{S \in \mathcal{S}_h^D} \frac{\mu}{|S|} \|\phi_h\|_{0,S}^2 \\ + a_{\rm stab}^{\rm NS}(\psi_h)(\psi_h) + \int_{\partial\Omega} \frac{\rho}{2} |\phi_{n,h}| \phi_h^2 + \int_{\Gamma^D} \theta_h^D \phi_{n,h}^2 + \int_{\Gamma^N} \theta_h^N \chi_h^2, \end{aligned} \tag{31}$$

where

$$A(\psi_h)(\psi_h) = a^{\rm S}(\psi_h, \psi_h) + \int_{\partial\Omega} \frac{\rho}{2} |\phi_{n,h}| \phi_h^2 - I_1(\psi_h, \phi_h) - I_2(\psi_h, \phi_h) + s(\phi_h, \phi_h).$$

Proof. By taking into account the estimate (26) for $A(\psi_h)(\psi_h)$, we only have to bound the terms on the Neumann boundary Γ^N:

$$\int_{\Gamma^N} \frac{\rho}{2} |\phi_{n,h}| \phi_h^2 + \int_{\Gamma^N} \theta_h^N \mathcal{C}(\psi_h)\mathcal{C}^{\rm adj}(\psi_h)(\psi_h).$$

By means of the relations $a^+ + a^- = a$, $a^+ - a^- = |a|$, $a^+ a^- = 0$ and $a^- a = (a^-)^2$, we have:

$$\begin{aligned} \mathcal{C}(\psi_h)\mathcal{C}^{\rm adj}(\psi_h)(\psi_h) =& \chi_h^2 + \chi_h(\rho \phi_{n,h}^2 + \frac{\rho}{2} {\rm sgn}(\phi_{n,h}) \phi_h^2) + \frac{\rho^2}{2} {\rm sgn}(\phi_{n,h}) (\phi_{n,h}^-)^2 \phi_h^2 \\ & - (\mu \partial_n \phi_h \cdot n)^2 - \mu \partial_n \phi_h \cdot n (\rho |\phi_{n,h}| \phi_{n,h} + \frac{\rho}{2} {\rm sgn}(\phi_{n,h}) \phi_h^2). \end{aligned}$$

Thanks to Young's inequality, we get:

$$\begin{aligned}\frac{\rho}{2}|\phi_{n,h}|\phi_h^2+\theta_h^N\mathcal{C}(\psi_h)\mathcal{C}^{\mathrm{adj}}(\psi_h)(\psi_h)\geq&\frac{\theta_h^N}{4}(4-\varepsilon)\chi_h^2-\frac{\theta_h^N}{4}(4+\delta)(\mu\partial_n\phi_h\cdot n)^2+\frac{\rho}{2}|\phi_{n,h}|\phi_h^2\\&-\frac{\theta_h^N}{2}\rho^2\phi_{n,h}^2\phi_h^2\\&-\frac{\theta_h^N}{\varepsilon}(\rho\phi_{n,h}^2+\frac{\rho}{2}\mathrm{sgn}(\phi_{n,h})\phi_h^2)^2\\&-\frac{\theta_h^N}{\delta}(\rho|\phi_{n,h}|\phi_{n,h}+\frac{\rho}{2}\mathrm{sgn}(\phi_{n,h})\phi_h^2)^2.\end{aligned}$$

After developing the last two terms and using the properties of the sign function, we get:

$$\begin{aligned}\frac{\rho}{2}|\phi_{n,h}|\phi_h^2+\theta_h^N\mathcal{C}(\psi_h)\mathcal{C}^{\mathrm{adj}}(\psi_h)(\psi_h)\geq&\frac{\theta_h^N}{4}(4-\varepsilon)\chi_h^2-\frac{\theta_h^N}{4}(4+\delta)(\mu\partial_n\phi_h\cdot n)^2+\frac{\rho}{2}|\phi_{n,h}|\phi_h^2\\&-\left(\frac{1}{\varepsilon}+\frac{1}{\delta}\right)\theta_h^N\rho^2\phi_{n,h}^4-\left(\frac{1}{\varepsilon}+\frac{1}{\delta}\right)\frac{\theta_h^N}{4}\rho^2\phi_h^4\\&-\left(\frac{1}{\varepsilon}+\frac{1}{\delta}+\frac{1}{2}\right)\theta_h^N\rho^2\phi_{n,h}^2\phi_h^2.\end{aligned}$$

We next use (30) and $|\phi_{n,h}|\leq|\phi_h|$ in order to bound the last three terms. Thus,

$$\begin{aligned}\frac{\rho}{2}|\phi_{n,h}|\phi_h^2-\left(\frac{1}{\varepsilon}+\frac{1}{\delta}\right)\theta_h^N\rho^2\phi_{n,h}^4-\left(\frac{1}{\varepsilon}+\frac{1}{\delta}\right)\frac{\theta_h^N}{4}\rho^2\phi_h^4-\left(\frac{1}{\varepsilon}+\frac{1}{\delta}+\frac{1}{2}\right)\theta_h^N\rho^2\phi_{n,h}^2\phi_h^2&\\\geq\left(\frac{1}{2}-\frac{1}{\gamma_4}(\frac{9}{4\varepsilon}+\frac{9}{4\delta}+\frac{1}{2})\right)\rho|\phi_{n,h}|\phi_h^2.&\end{aligned}$$

We now choose $0<\varepsilon<4$, $0<\delta$ and $\gamma_4>1+9\left(1/\varepsilon+1/\delta\right)/2$, for instance $\varepsilon=\delta=2$ and $\gamma_4>11/2$. We also use (29) and we get point-wise, on any side $S\subset\Gamma^N$, that:

$$\frac{\rho}{2}|\phi_{n,h}|\phi_h^2+\theta_h^N\mathcal{C}(\psi_h)\mathcal{C}^{\mathrm{adj}}(\psi_h)(\psi_h)\geq\frac{\theta_h^N}{2}\chi_h^2+\frac{2\gamma_4-11}{4\gamma_4}\rho|\phi_{n,h}|\phi_h^2-\frac{3|S|}{2\gamma_3}\mu(\partial_n\phi_h\cdot n)^2.$$

The last term, which is negative, is controlled for γ_3 sufficiently large as usually in Nitsche's method, by means of the discrete inequality:

$$\sum_{S\in\mathcal{S}_h^N}|S|\int_S\mu(\partial_n\phi_h\cdot n)^2\lesssim\mu|\phi_h|_{1,\Omega}^2.$$

We have thus established the coercivity (31). □

Let us next focus on the drag error, for the following discrete formulation: find $u_h=(v_h,p_h)\in V_h\times M_h$,

$$\begin{aligned}(a^{\mathrm{NS}}+a^{\mathrm{NS}}_{\mathrm{stab}}+s^\partial)(u_h)(\psi_h)-I_1(u_h,\phi_h)-I_2(\psi_h,v_h-v^D)+s(v_h-v^D,\phi_h)&\\=l^{\mathrm{NS}}(u_h)(\psi_h),\qquad\forall\psi_h=(\phi_h,\chi_h)\in V_h\times M_h.&\end{aligned}$$

Exactly as in subsection 3.1, we have that

$$J^{\mathrm{S}}(u_h)-J(u)=\mathcal{T}^{\mathrm{S}}+\mathcal{T}^{\mathrm{c}}+\mathcal{T}^{\mathrm{lin}}+\mathcal{T}^{\mathrm{rhs}}+\mathcal{T}^{\mathrm{adj}}+\mathcal{T}^{\mathrm{stab}}+s^\partial(u_h)(\mathcal{L}_hz).$$

By decomposing s^∂ as s^N+s^D with obvious notation, we can write that:

$$s^\partial(u_h)(\mathcal{L}_hz)=s^N(u_h)(\mathcal{L}_hz)+\int_\Sigma\theta_h^D(v_{n,h}-v_n^D)n\cdot e_1.$$

So, by defining the new discrete drag as follows:

$$J^{\mathrm{NS}}(u_h) = \tilde{J}^{\mathrm{NS}}(u_h) - \int_\Sigma \theta_h^D (v_{n,h} - v_n^D) n \cdot e_1, \tag{32}$$

we get:

$$J^{\mathrm{NS}}(u_h) - J(u) = \mathcal{T}^{\mathrm{h.o.t.}} + \mathcal{T}^N + s^N(u_h)(\mathcal{L}_h z).$$

Theorem 4. *Under the assumptions (17), (18) and (19), one has that*

$$|J^{\mathrm{NS}}(u_h) - J(u)| \leq c\, h^2.$$

Proof. Thanks to Theorem 2, we only have to bound $s^N(u_h)(\mathcal{L}_h z)$. Using that $\mathcal{C}(u) = p^N$ and that $\mathcal{C}^{\mathrm{adj}}(u)(z) = 0$, we can write that:

$$\begin{aligned} s^N(u_h)(\mathcal{L}_h z) &= \int_{\Gamma^N} \theta_h^N (\mathcal{C}(u_h) - p^N) \mathcal{C}^{\mathrm{adj}}(u_h)(\mathcal{L}_h z) \\ &= \int_{\Gamma^N} \theta_h^N \Big(\mathcal{C}(u_h) - \mathcal{C}(u) \Big) \Big(\mathcal{C}^{\mathrm{adj}}(u_h)(\mathcal{L}_h z - z) + \mathcal{C}^{\mathrm{adj}}(u_h)(z) - \mathcal{C}^{\mathrm{adj}}(u)(z) \Big). \end{aligned}$$

Thanks to the Cauchy-Schwarz inequality, we immediately get:

$$\begin{aligned} |s^N(u_h)(\mathcal{L}_h z)| \leq \sqrt{2} \Bigg(& \sum_{S \in \mathcal{S}_h^N} |\theta_h^N|_{\infty,S} \|\mathcal{C}(u_h) - \mathcal{C}(u)\|_{0,S}^2 \Bigg)^{1/2} \\ & \Bigg(\sum_{S \in \mathcal{S}_h^N} |\theta_h^N|_{\infty,S} \|\mathcal{C}^{\mathrm{adj}}(u_h)(\mathcal{L}_h z - z)\|_{0,S}^2 \\ & + \sum_{S \in \mathcal{S}_h^N} ||\theta_h^N|_{\infty,S} \|\mathcal{C}^{\mathrm{adj}}(u_h)(z) - \mathcal{C}^{\mathrm{adj}}(u)(z)\|_{0,S}^2 \Bigg)^{1/2}. \end{aligned} \tag{33}$$

Let $S \in \mathcal{S}_h^N$ and $K \in \mathcal{K}_h$ such that $S \subset \partial K$. In order to estimate the $L^2(S)$-norm of $\mathcal{C}(u_h) - \mathcal{C}(u)$, we use several ingredients: the estimate

$$|a^- a - b^- b| = |(a^- - b^-)(a^- + b^-)| \leq |a - b|(|a| + |b|),$$

the following inequality between discrete norms:

$$\|v_h\|_{\infty,S} \lesssim |v_h|_{1,K} + |S|^{-1/2} \|v_h\|_{0,S} \lesssim |v_h|_{1,\Omega} + |S|^{-1/2} \|v_h\|_{0,\Gamma^N} \lesssim |S|^{-1/2} \|v_h\|_{1,\Omega}, \tag{34}$$

as well as the estimate $\|v\|_{\infty,S} \leq \|v\|_{\infty,\Gamma^N} \lesssim \|v\|_{2,\Omega}$, the latter resulting from the Sobolev embedding theorem applied to $v \in H^2(\Omega)^2$. Then we get:

$$\begin{aligned} \|\mathcal{C}(u_h) - \mathcal{C}(u)\|_{0,S} \lesssim & (\|v_h\|_{\infty,S} + \|v\|_{\infty,S}) \|v_n - v_{n,h}\|_{0,S} + \|\mu \partial_n (v - v_h) \cdot n - (p - p_h)\|_{0,S} \\ \lesssim & |S|^{-1/2} \|v - v_h\|_{0,S} + \|\mu \partial_n (v - v_h) \cdot n - (p - p_h)\|_{0,S}. \end{aligned}$$

The trace inequality and the discrete inequality $|S|^{1/2} \|p_h - \mathcal{L}_h p\|_{0,S} \lesssim \|p_h - \mathcal{L}_h p\|_{0,K}$ give:

$$\begin{aligned} |S|^{1/2} \|\partial_n (v - v_h)\|_{0,S} \lesssim & \left(|v - v_h|_{1,K} + d_K |v|_{2,K} \right), \\ |S|^{1/2} \|p - p_h\|_{0,S} \lesssim & \|p_h - \mathcal{L}_h p\|_{0,K} + \|p - \mathcal{L}_h p\|_{0,K} + d_K |p - \mathcal{L}_h p|_{1,K} \\ \lesssim & \|p_h - p\|_{0,K} + \|p - \mathcal{L}_h p\|_{0,K} + d_K |p|_{1,K}. \end{aligned}$$

Thanks to the approximation and interpolation errors and to (29), we can conclude that:

$$\left(\sum_{S\in\mathcal{S}_h^N} |\theta_h^N|_{\infty,S}\|\mathcal{C}(u_h)-\mathcal{C}(u)\|_{0,S}^2\right)^{1/2} \leq ch.$$

By using the same estimate (34) as previously for $\|v_h\|_{\infty,S}$, the trace inequality and the interpolation error, we obtain similarly to Section 2 that:

$$\begin{aligned}\|\mathcal{C}^{\mathrm{adj}}(u_h)(\mathcal{L}_h z - z)\|_{0,S} \lesssim & \|v_h\|_{\infty,S}\|\mathcal{L}_h z_v - z_v\|_{0,S} + \|\mu\partial_n(\mathcal{L}_h z_v - z_v)\cdot n + \mathcal{L}_h z_p - z_p\|_{0,S}\\ \lesssim & |S|^{1/2}(|z_v|_{2,K} + |z_p|_{1,\omega_K}).\end{aligned}$$

The inequality (29) next yields:

$$\left(\sum_{S\in\mathcal{S}_h^N} \theta_h^N\|\mathcal{C}^{\mathrm{adj}}(u_h)(\mathcal{L}_h z - z)\|_{0,S}^2\right)^{1/2} \leq ch.$$

In order to bound the remaining term of (33), let us first note that

$$\mathcal{C}^{\mathrm{adj}}(u_h)(z) - \mathcal{C}^{\mathrm{adj}}(u)(z) = \rho(v_{n,h}^+ - v_n^+)z_v\cdot n + \frac{\rho}{2}\left(\mathrm{sgn}(v_{n,h})v_h - \mathrm{sgn}(v_n)v\right)\cdot z_v.$$

By using the inequalities (29) and $|a^+ - b^+| \leq |a-b|$, we first get that:

$$\left(\sum_{S\in\mathcal{S}_h^N} \theta_h^N\|\rho(v_{n,h}^+ - v_n^+)z_v\cdot n\|_{0,S}^2\right)^{1/2} \lesssim \left(\sum_{S\in\mathcal{S}_h^N} |S|\|v_h - v\|_{0,S}^2\right)^{1/2} \|z_v\|_{\infty,\Gamma^N}.$$

By using next the trace theorem in Ω, the $H^1(\Omega)$-approximation error for $v_h - v$ and Sobolev's theorem applied to $z_v \in H^2(\Omega)^2$, we further obtain:

$$\left(\sum_{S\in\mathcal{S}_h^N} \theta_h^N\|\rho(v_{n,h}^+ - v_n^+)z_v\cdot n\|_{0,S}^2\right)^{1/2} \lesssim \sqrt{h}\|v_h - v\|_{0,\Gamma^N}\|z_v\|_{2,\Omega} \leq ch.$$

Similarly, hypothesis (**??**) leads to:

$$\begin{aligned}\left(\sum_{S\in\mathcal{S}_h^N} \theta_h^N\|\frac{\rho}{2}\left(\mathrm{sgn}(v_{n,h})v_h - \mathrm{sgn}(v_n)v\right)\cdot z_v\|_{0,S}^2\right)^{1/2} &\leq \left(\sum_{S\in\mathcal{S}_h^N} \theta_h^N\|\frac{\rho}{2}(v_h - v)\cdot z_v\|_{0,S}^2\right)^{1/2}\\ &\lesssim \sqrt{h}\|v_h - v\|_{0,\Gamma^N}\|z_v\|_{\infty,\Gamma^N} \leq ch.\end{aligned}$$

Finally, by gathering together the previous estimates we deduce from (33) the desired result, that is:

$$|s^N(u_h)(\mathcal{L}_h z)| \leq ch^2.$$

□

4. Numerical results

In this section, we present some numerical experiments illustrating the theoretical results, carried out by using a in-house C++ library. We consider here quadrilateral meshes. For the convergence analysis, we use successive meshes obtained by uniform refinement.

We present two test-cases for which we dispose of a reference drag value. The first test-case uses manufactured exact solutions for Stokes and Navier-Stokes equations, while the second one is the well-known cylinder benchmark of [26] for the Navier-Stokes equations. Finally, we apply our approach to a time-dependent flow considered in the cylinder benchmark and compare our results with the literature. For all considered examples, we have taken $e_1 = (1, 0)$.

Table 1: $(Q_1)^2 \times Q_1$ Stokes case: errors, drag and convergence orders

N	$\|p - p_h\|_{0,\Omega}$	r	$\|v - v_h\|_{1,\Omega}$	r	$\|v - v_h\|_{0,\Omega}$	r	drag	r
64	4.72e-03	–	4.97e-01	–	1.78e-02	–	0.1289250	–
256	1.51e-03	1.64	2.48e-01	1.01	4.48e-02	1.99	0.1123778	1.97
1 024	5.08e-04	1.58	1.24e-01	1.00	1.12e-03	2.00	0.1081210	1.97
4 096	1.75e-04	1.54	6.18e-02	1.00	2.81e-03	2.00	0.1070358	1.98
16 384	6.10e-05	1.52	3.09e-02	1.00	7.04e-04	2.00	0.1067602	1.98
65 536	2.14e-05	1.51	1.54e-02	1.00	1.76e-04	2.00	0.1066903	1.98

Table 2: $(Q_1)^2 \times Q_1$ Stokes case: drag error without correction term

N	$\|J(u) - J(u_h)\|$	r
64	0.0624974	–
256	0.0208485	1.58
1 024	0.0077612	1.43
4 096	0.0032150	1.27
16 384	0.0014333	1.17

4.1. Exact solutions

We use the computational domain $\Omega = [0,1]^2$ and prescribe the data such that the exact solution is given by:

$$v(x,y) = \left(4y(1-y^2)(1-x^2)^2, -4x(1-x^2)^2(1-y^2)^2\right), \qquad p(x,y) = x^3 - y^3.$$

We impose a homogeneous Dirichlet condition on the upper ($y = 1$) and the right ($x = 1$) boundaries and a non-homogeneous Dirichlet condition on the left boundary ($x = 0$), whereas on the lower boundary ($y = 0$) an outflow condition (9) is imposed. Note that the latter corresponds to a standard Neumann condition, since $v_n^- = 0$. The viscosity is taken equal to $\mu = 0.025$.

We compute the drag value on the upper boundary and we compare the obtained approximation to its exact value, equal to $8/75 = 0.10(6)$.

We begin by considering the Stokes system, solved by using the $(Q_1)^2 \times Q_1$ stabilized discretization of Section 2. Table 1 gathers the H^1 and L^2-norms of the velocity error, the L^2-norm of the pressure error and the computed values of the drag, on successive meshes. The first column of the table gives the number of cells N on the different meshes. The columns titled by r indicate the corresponding convergence rates. We note that we numerically retrieve the optimal convergence order $O(h^2)$ for the drag error, proved in Section 2.

Remark 6. *The correction term $J^{\mathrm{S}}(u_h) - J(u_h)$ resulting from Nitsche's stabilization is essential in order to obtain the $O(h^2)$ convergence rate for the drag error. Table 2 shows that without such a correction, the convergence order decreases to $O(h)$.*

We next consider the Navier-Stokes system with the same analytical solution, boundary conditions and viscosity as before. The numerical results obtained by the $(Q_1)^2 \times Q_1$ method of Section 3 (including SUPG and boundary stabilization) are shown in Table 3.

We remark that we get the same convergence rates as in the Stokes case, which are those predicted by the theory.

Table 3: $(Q_1)^2 \times Q_1$ Navier-Stokes case: errors, drag and convergence orders

N	$\|p - p_h\|_{0,\Omega}$	r	$\|v - v_h\|_{1,\Omega}$	r	$\|v - v_h\|_{0,\Omega}$	r	drag	r
64	5.97e-03	–	5.00e-01	–	1.48e-02	–	0.1282372	–
256	2.18e-03	1.45	2.47e-01	1.00	4.23e-03	1.80	0.1121847	1.97
1 024	7.10e-04	1.62	1.24e-01	1.00	1.14e-03	1.89	0.1080739	1.97
4 096	2.17e-04	1.71	6.18e-02	1.00	2.94e-03	1.96	0.1070244	1.98
16 384	6.72e-05	1.69	3.09e-02	1.00	7.43e-04	1.99	0.1067574	1.98
65 536	2.18e-05	1.63	1.54e-02	1.00	1.86e-04	2.00	0.1066896	1.98

4.2. Cylinder benchmark

We now consider the benchmark of [26] describing the flow over a circular cylinder; it models a fluid flow in a pipe with a circular obstacle. We compute the drag on the obstacle's boundary, denoted by Σ.

4.2.1. Steady case

The considered geometry for the pipe is the rectangle $\Omega = [0, 2.2] \times [0, 0.41]$ and the obstacle is a circle centred at $(0.2, 0.2)$ of radius 0.05, see Figure 1. The fluid viscosity is taken equal to $\mu = 0.001$, which yields a Reynolds number equal to 20.

We set the following boundary conditions:

- On the lower and upper walls as well as on the obstacle's boundary, no-slip boundary conditions are imposed. So, by putting $\Gamma_{\text{wall}} = [0, 2.2] \times \{0\} \cup [0, 2.2] \times \{0.41\} \cup \Sigma$, we have $v_{|\Gamma_{\text{wall}}} = 0$.
- On the left boundary $\Gamma_{\text{in}} = \{0\} \times [0, 0.41]$ a parabolic inflow profile is prescribed,

$$v(0, y) = \frac{4v_{\max}}{0.41^2}(y(0.41 - y), 0) \tag{35}$$

  with $v_{\max} = 0.3$.
- Finally, on the right boundary $\Gamma_{\text{out}} = \{2.2\} \times [0, 0.41]$, one imposes the outflow condition

$$\mu \partial_n v - pn = 0. \tag{36}$$

Thus, we have that $\Gamma^D = \Gamma_{\text{wall}} \cup \Gamma_{\text{in}}$ and $\Gamma^N = \Gamma_{\text{out}}$. Note that for this benchmark, it is known that there is no recirculation on Γ_{out} (that is, $v_n^- = 0$ on Γ_{out}), and thus our outflow condition (9) is equivalent to (36). The drag is computed on Σ and compared to the reference value $J = 5.57953523384$, cf. for instance [23], [21].

Figure 1: Geometry and boundary conditions for the cylinder benchmark

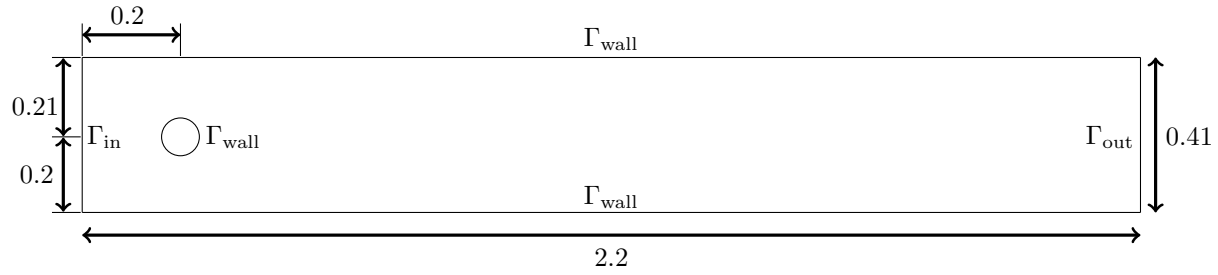

Figure 2: Cylinder benchmark: quadrilateral mesh with 2560 cells

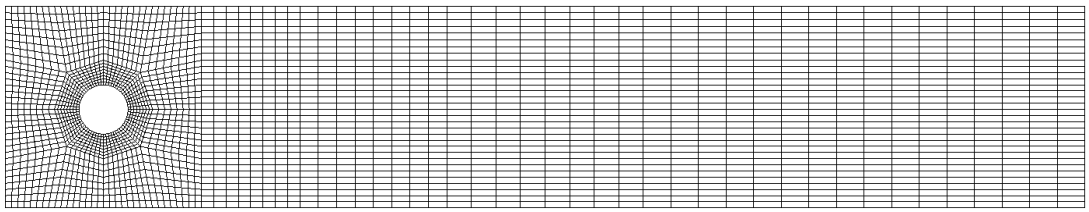

Figure 2 shows an intermediate mesh, while Figure 3 shows the pressure isolines obtained by a fully stabilized $(Q_1)^2 \times Q_1$ finite element method. Table 4 presents the corresponding drag values together with the convergence orders and the relative errors; the first two columns give the number of cells and the number of degrees of freedom, respectively.

We note that we numerically obtain the optimal convergence rate $O(h^2)$ for the drag error, as predicted by the theory.

We couldn't find in the literature the drag computation for this benchmark by means of stabilized $(Q_1)^2 \times Q_1$ finite elements. However, we can note that our method yields the same convergence order as the nonconforming $(Q_1^{rot})^2 \times Q_0$ method, see [21] as well as Appendix B. Although these two low-order finite element methods yield the same convergence order, it is well-known that they don't have similar computational costs. In Tables 4 and 5, one can see that on the same mesh, the relative error is approximately 4 times larger and the number of degrees of freedom is approximately 1.6 times larger for the nonconforming method. A similar behaviour is observed in [21], when comparing nonconforming and conforming methods.

Figure 3: $(Q_1)^2 \times Q_1$ cylinder benchmark solution: isolines of pressure

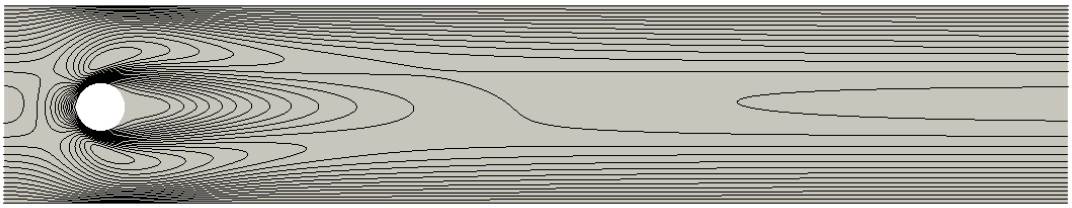

Table 4: Drag computation with the $(Q_1)^2 \times Q_1$ method for the cylinder benchmark

N	d.o.f.	drag	r	relative error
640	2 124	5.657508833113	–	0.0139749
2 560	8 088	5.593347524445	2.4970331	0.0024755
10 240	31 536	5.582312273511	2.3143329	0.0004977
40 960	124 512	5.580168154540	2.1334511	0.0001134
163 840	494 784	5.579689329110	2.0382022	0.0000276

4.2.2. Cut domain

We now test the influence of the modified outflow condition. We recall that in the previous test-case, the flow on Γ_{out} is outgoing. In order to have a re-entrant flow on the outflow boundary, we have increased the inflow velocity to $v_{\max} = 1$ in (35), and cut the domain behind the cylinder, at $x = 0.4$. Figure 4 shows the velocity streamlines in the whole domain, whereas in Figure 5 we compare in the same domain

Table 5: Drag computation with the $(Q_1^{rot})^2 \times Q_0$ method for the cylinder benchmark

N	d.o.f.	drag	r	relative error
640	3 336	5.857557058537	–	0.049828850
2 560	13 072	5.635208719813	2.32	0.009978158
10 240	51 744	5.590669151087	2.32	0.001995492
40 960	205 888	5.582009694953	2.17	0.000443489
163 840	821 376	5.580119287786	2.08	0.000104678

Ω_{cut} the streamlines of the velocity computed in the whole domain with those computed in the cut domain (hence, with the modified outflow condition). Table 6 shows the drag coefficients in the two cases, on a sequence of refined meshes. As expected, the values are close to each other but not identical, since we have modified the model problem by cutting the domain near the cylinder. We cannot study the numerical convergence order for the drag on the cut domain since we do not dispose of a reference value for this domain.

Figure 4: Flow around a cylinder with increased inflow velocity: streamlines

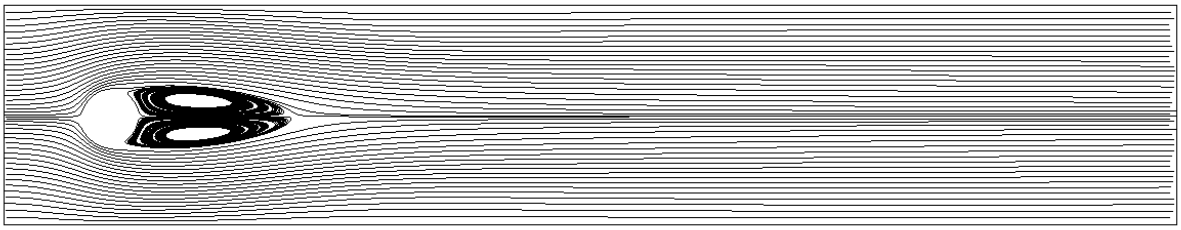

Figure 5: Comparison in Ω_{cut} of velocity streamlines: whole (left) and cut (right) domains

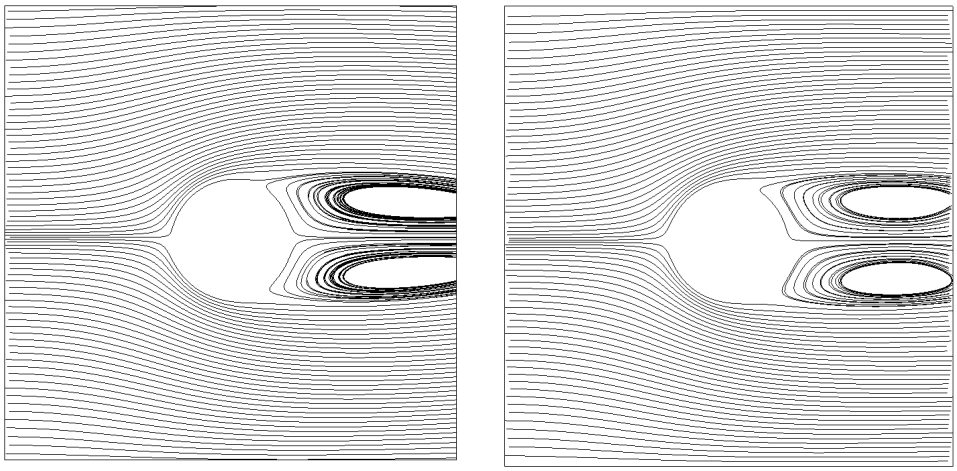

4.2.3. Unsteady case

Finally, we test our approach in the case of unsteady flows. The stabilized finite element method employed in this work can also be used for time-dependent flows, with stabilization parameters θ which depend on the time step (see [7], [8]). We consider here the cylinder benchmark configuration of the previous subsection, but with an increased inflow velocity $v_{\max} = 1.5$. This yields a Reynolds number

Table 6: Comparison of drag values for the whole and cut domains

$N(\Omega)$	drag on Ω	$N(\Omega_{\text{cut}})$	drag on Ω_{cut}
640	1.537335646447	320	1.515744677887
2 560	1.490398932070	1 280	1.466342063137
10 240	1.483690048328	5 120	1.459151131886
40 960	1.481798249598	20 480	1.457154672672

Table 7: Comparison of minimum and maximum drag values for unsteady flow

method	d.o.f.	min	max
reference value	667 264	3.1569	3.2200
$(Q_2)^2 \times P_1^{disc}$	10 608	3.0992	3.1624
$(Q_2)^2 \times P_1^{disc}$	42 016	3.1333	3.1958
$(Q_1)^2 \times Q_1$	8 088	3.1625	3.2301
$(Q_1)^2 \times Q_1$	31 536	3.1580	3.2178

equal to 100 and a periodic developed flow. This test-case was also used in [18] for the drag computation with an isogeometric method based on NURBS appproximation.

Figure 6: Time-dependent flow around a cylinder: velocity magnitude

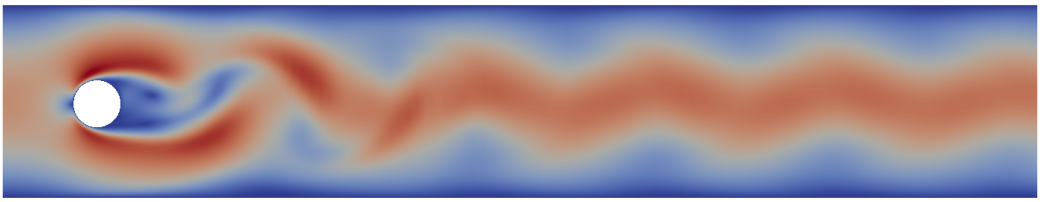

The velocity magnitude computed with our method is shown in Figure 6. In Figure 7, we compare the computed drag over time obtained with our stabilized $(Q_1)^2 \times Q_1$ method on two levels of mesh refinement, with the drag obtained in [27], [22] with a $(Q_2)^2 \times P_1^{disc}$ finite element method on two meshes. The reference value is the one computed on a refined mesh with 667 264 degrees of freedom, cf. [22]. First, we note that our results are in very good agreement with the reference value. Second, we can also note that we obtain better results than in [27] when using much less degrees of freedom. We also show in Table 7 the minimum and maximum drag values obtained with the two finite element methods on different meshes, for $\Delta t = 1/400$.

5. Concluding remarks

We have considered stabilized $(P_1)^2 \times P_1$ and $(Q_1)^2 \times Q_1$ continuous finite elements for the discretization of the Stokes and the Navier-Stokes equations. The corresponding formulation presents interesting numerical properties, as mentioned in the introduction.

We have focused on the computation of the drag, in particular on the convergence order. Several numerical tests in the literature highlight an improved $O(h^{2k})$ convergence rate for the drag error when using a $O(h^k)$ approximation method, see for instance [21], [18].

In this paper, we have proved such a result. For this purpose, we have introduced a corrected drag, which takes into account the different stabilization terms on the obstacle's boundary, and we have used a

Figure 7: Comparison of drag for a time-dependent flow around cylinder

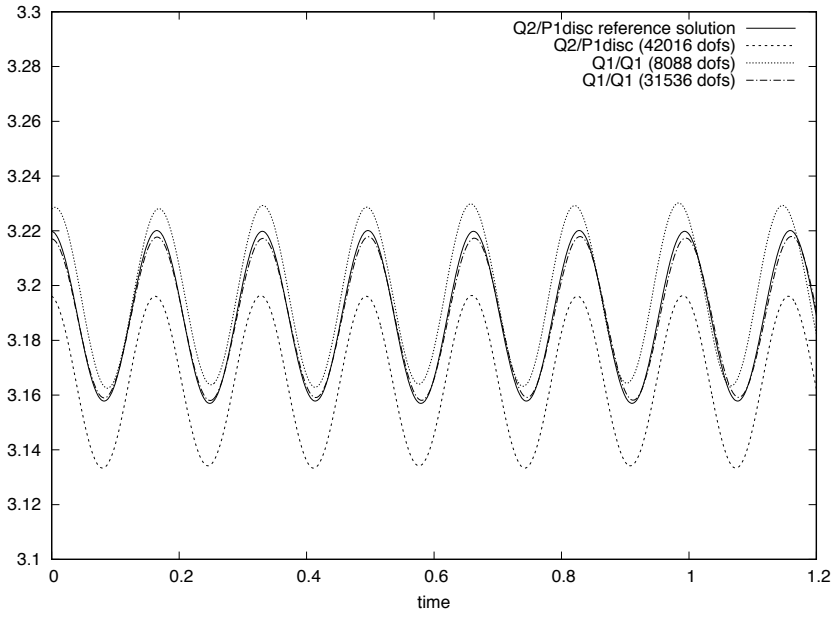

duality argument. We have noted that the addition of correction terms to the discrete drag is necessary, which leads us to believe that this should be the case for other stabilized methods, too. The theoretical results are confirmed by numerical experiments.

Finally, the duality technique employed in this work can be applied to other finite element methods for the Navier-Stokes equations. In the appendices, we consider two well-known inf-sup stable schemes, which use the conforming Taylor-Hood elements and the nonconforming Crouzeix-Raviart or Rannacher-Turek elements. We deduce again the improved convergence rate for the drag error.

Appendix A. Conforming $(P_2)^2 \times P_1$ or $(Q_2)^2 \times Q_1$ discretizations

We consider Lagrange finite elements of degree 2 for the velocity and 1 for the pressure, on either triangular or quadrilateral meshes. This pair yields a conforming inf-sup stable approximation of the Navier-Stokes equations, and therefore can be used without any SUPG stabilization, at least for Reynolds numbers which are not too large. In what follows, we take

$$a_{\text{stab}}^{\text{NS}} = s^{\partial} = 0. \tag{A.1}$$

For $u \in H^{m+1}(\Omega)^2 \times H^m(\Omega)$ with $1 \leq m \leq 2$, one has

$$|||u - u_h||| \leq ch^m.$$

In order to study the convergence of the drag error, we use the same process as previously in Section 3. We define the drag value by (22). Note that, since no stabilization is used now, we have in this case

$$\begin{aligned} J^{\text{NS}}(u_h) = \tilde{J}^{\text{NS}}(u_h) = &\int_{\Sigma} (\mu \partial_n v_h - p_h n) \cdot e_1 - \sum_{S \subset \Sigma} \int_S \frac{\gamma_1 \mu}{|S|} (v_h - v^D) \cdot e_1 \\ &- \int_{\Sigma} \frac{\rho}{2} (v_{n,h} - v_n^D) v^D \cdot e_1 + \rho (v_n^D)^+ (v_h - v^D) \cdot e_1. \end{aligned} \tag{A.2}$$

We obtain the expression (23) for the drag error, with $\mathcal{T}^{\rm stab} = 0$. Under the hypotheses $\mathrm{sgn}(v_n) = \mathrm{sgn}(v_{n,h})$ on Γ^N and $z \in H^{l+1}(\Omega)^2 \times H^l(\Omega)$ with $1 \le l \le 2$, it follows thanks to the interpolation and the approximation error estimates that

$$|J(u) - J^{\rm NS}(u_h)| \le ch^{m+l}.$$

The optimal convergence rate $O(h^4)$ is obtained for $m = l = 2$. Note that in practice, the regularity of the adjoint problem often limits the convergence rate of the drag error.

As explained in subsection 3.2, it is useful to stabilize the boundary conditions. Adding the term s^∂ to the discrete formulation does not change the previous convergence rate $O(h^{m+l})$ of the drag, which is now defined by (32).

Appendix B. Nonconforming $(P_1)^2 \times P_0$ and $(Q_1^{rot})^2 \times Q_0$ discretizations

We consider nonconforming finite elements of degree 1 for the velocity: Crouzeix-Raviart elements [16] on triangles, Rannacher-Turek elements [25] on quadrilaterals. In both cases, we have:

$$\int_S [v_h] = 0, \quad \forall S \in \mathcal{S}_h^{int}, \quad \forall v_h \in V_h. \tag{B.1}$$

The pressure is approximated by means of piecewise constant elements. It is well-known that the pairs (V_h, M_h) are inf-sup stable and yield the following error estimate, for $u = (v, p) \in H^2(\Omega)^2 \times H^1(\Omega)$:

$$|||u - u_h|||_h \le ch,$$

where $|||\cdot|||_h$ is defined by using the $H^1(\Omega)$ broken semi-norm in the definition of $|||\cdot|||$. In the following, we consider again (A.1), which yields the same expression (A.2) for the discrete drag as for the Taylor-Hood elements. We also have $\mathcal{T}^{\rm stab} = 0$.

Lemma 4. *One has that*

$$J^{\rm NS}(u_h) - J(u) = \mathcal{T}^{\rm h.o.t.} + \mathcal{T}^N + \mathcal{T}^{\rm ncf}, \tag{B.2}$$

where the additional term $\mathcal{T}^{\rm ncf}$ is defined by:

$$\mathcal{T}^{\rm ncf} = \sum_{S \in \mathcal{S}_h^{int}} \int_S (\frac{\rho}{2} v_n z_v + \mu \partial_n z_v + z_p n) \cdot [v_h] + \sum_{S \in \mathcal{S}_h^{int}} \int_S (\frac{\rho}{2} v_n v - \mu \partial_n v + pn) \cdot [z_v - \mathcal{L}_h z_v].$$

Proof. We use the discrete problem with the test-function $\mathcal{L}_h z$, but, contrarily to subsection 3.1, we test (10) with $\psi = z$. We thus obtain:

$$J^{\rm S}(u_h) - J(u) = \mathcal{T}^{\rm S} + \mathcal{T}^{\rm c} + \mathcal{T}^{\rm lin} + \mathcal{T}^{\rm rhs} + \mathcal{T}^{\rm adj} + l^{\rm NS}(u)(z - \mathcal{L}_h z) - a^{\rm NS}(u)(z - \mathcal{L}_h z). \tag{B.3}$$

The terms $\mathcal{T}^{\rm S}$, $\mathcal{T}^{\rm c}$, $\mathcal{T}^{\rm lin}$ and $\mathcal{T}^{\rm rhs}$ are bounded exactly as in subsection 3.1, since no integration by parts is needed in order to estimate them.

As regards the term $\mathcal{T}^{\rm adj}$, we first use the relation (14) with $\eta = u$ in order to obtain:

$$\mathcal{T}^{\rm adj} = (a^{\rm NS})'_u(u_h, z) - I_2(z, v_h) - \int_{\Gamma^D} \rho v_n^+ v \cdot z_v + \frac{\rho}{2} \mathrm{sgn}(v_n) v_n v \cdot z_v.$$

Then we perform an integration by parts with respect to z and we use the adjoint boundary value problem (12) with the boundary condition (13). This yields:

$$\begin{aligned}
\mathcal{T}^{\rm adj} = & \sum_{S \in \mathcal{S}_h^{int} \cup \mathcal{S}_h^D} \int_S (\mu \partial_n z_v + z_p n + \frac{\rho}{2} v_n z_v) \cdot [v_h] + \int_\Sigma \frac{\rho}{2} \left(\mathrm{sgn}(v_n^D) v_{n,h} v^D + \left| v_n^D \right| v_h \right) \cdot e_1 \\
& - \int_{\Gamma^D} (\mu \partial_n z_v + z_p n) \cdot v_h - \int_\Sigma \rho (v_n^D)^+ v^D \cdot e_1 + \frac{\rho}{2} \mathrm{sgn}(v_n^D) v_n^D v^D \cdot e_1 \\
= & \int_\Sigma \rho (v_n^D)^+ (v_h - v^D) \cdot e_1 + \frac{\rho}{2} \mathrm{sgn}(v_n^D)(v_{n,h} - v_n^D) v^D \cdot e_1 + \sum_{S \in \mathcal{S}_h^{int}} \int_S (\mu \partial_n z_v + z_p n + \frac{\rho}{2} v_n z_v) \cdot [v_h].
\end{aligned}$$

Here above, we have used that $v_n^D + |v_n^D| = 2(v_n^D)^+$ on Γ^D.

The additional consistency term in (B.3) is treated by integrating with respect to u and by using the boundary value problem (8) with the outflow condition (9), and the fact that $z_v = \xi = \mathcal{L}_h z_v$ on Γ^D. Noting that

$$\int_\Omega \frac{\rho}{2} v \cdot (v \cdot \nabla(z_v - \mathcal{L}_h z_v)) = -\int_\Omega \frac{\rho}{2}(v \cdot \nabla v) \cdot (z_v - \mathcal{L}_h z_v) + \sum_{S \in \mathcal{S}_h} \int_S \frac{\rho}{2} v_n v \cdot [z_v - \mathcal{L}_h z_v]$$

and using $v_n - |v_n| = 2v_n^-$ on Γ^N, we finally obtain that:

$$l^{\rm NS}(u)(z - \mathcal{L}_h z) - a^{\rm NS}(u)(z - \mathcal{L}_h z) = \sum_{S \in \mathcal{S}_h^{int}} \int_S (\frac{\rho}{2} v_n v - \mu \partial_n v + pn) \cdot [z_v - \mathcal{L}_h z_v].$$

Summing up the previous contributions and using the notation introduced in (21) and (22) yield the announced result (B.2). □

Lemma 5. *Under the regularity assumptions (17) and (19), one has that*

$$|\mathcal{T}^{\rm ncf}| \le ch^2.$$

Proof. For any interior side $S \in \mathcal{S}_h^{int}$, the integral $\displaystyle\int_S (\frac{\rho}{2} v_n v - \mu \partial_n v + pn) \cdot [z_v - \mathcal{L}_h z_v]$ is bounded as usually when dealing with nonconforming methods. That is, the relation (B.1) and the continuity of z_v across S allow us to subtract an arbitrary constant vector to $\displaystyle\frac{\rho}{2} v_n v - \mu \partial_n v + pn = \Big(\frac{\rho}{2} v \otimes v - \mu \nabla v + pI\Big) n$. By subtracting $C_S n$ with the matrix $C_S = \pi_S^0 \Big(\frac{\rho}{2} v \otimes v - \mu \nabla v + pI\Big)$, we get:

$$\begin{aligned}
&|\sum_{S \in \mathcal{S}_h^{int}} \int_S (\frac{\rho}{2} v_n v - \mu \partial_n v + pn) \cdot [z_v - \mathcal{L}_h z_v]| \\
&\le \Big(\sum_{S \in \mathcal{S}_h^{int}} \frac{|S|}{\mu} \| \Big(\frac{\rho}{2} v \otimes v - \mu \nabla v + pI - C_S\Big) n \|_{0,S}^2 \Big)^{1/2} \Big(\sum_{S \in \mathcal{S}_h^{int}} \frac{\mu}{|S|} \|[z_v - \mathcal{L}_h z_v]\|_{0,S}^2 \Big)^{1/2} \\
&\lesssim \Big(\sum_{K \in \mathcal{K}_h} \frac{d_K^2}{\mu} |\frac{\rho}{2} v \otimes v - \mu \nabla v + pI|_{1,K}^2 \Big)^{1/2} \Big(\sum_{K \in \mathcal{K}_h} \frac{\mu}{d_K^2} \|z_v - \mathcal{L}_h z_v\|_{0,K}^2 + \mu |z_v - \mathcal{L}_h z_v|_{1,K}^2 \Big)^{1/2} \le ch^2.
\end{aligned}$$

As regards the remaining term in $\mathcal{T}^{\rm ncf}$, we similarly get that:

$$\begin{aligned}
&|\sum_{S \in \mathcal{S}_h^{int}} \int_S (\frac{\rho}{2} v_n z_v + \mu \partial_n z_v + z_p n) \cdot [v_h]| \\
&\le \Big(\sum_{K \in \mathcal{K}_h} \frac{d_K^2}{\mu} |\frac{\rho}{2} z_v \otimes v + \mu \nabla z_v + z_p I|_{1,K}^2 \Big)^{1/2} \Big(\sum_{S \in \mathcal{S}_h^{int}} \frac{\mu}{|S|} \|[v_h]\|_{0,S}^2 \Big)^{1/2} \\
&\lesssim h \Big(\sum_{S \in \mathcal{S}_h^{int}} \frac{\mu}{|S|} \|[v_h - \mathcal{I}_h^c v]\|_{0,S}^2 \Big)^{1/2},
\end{aligned}$$

with $\mathcal{I}_h^c v$ the P_1-continuous or Q_1-continuous interpolate of v. We next use the standard inequality on any interior side $S = \partial K^{in} \cap \partial K^{ex}$:

$$\frac{1}{\sqrt{|S|}} \|[v_h - \mathcal{I}_h^c v]\|_{0,S} \lesssim \big(|v_h - \mathcal{I}_h^c v|_{1,K^{in}} + |v_h - \mathcal{I}_h^c v|_{1,K^{ex}} \big)$$

and we obtain, by means of the triangle inequality,

$$\sum_{S\in\mathcal{S}_h^{int}} \frac{\mu}{|S|}\|[v_h - \mathcal{I}_h^c v]\|_{0,S}^2 \lesssim \left(\mu|v-\mathcal{I}_h^c v|_{1,\Omega}^2 + \sum_{K\in\mathcal{K}_h} \mu|v-v_h|_{1,K}^2\right).$$

This finally yields

$$|\sum_{S\in\mathcal{S}_h^{int}} \int_S (\frac{\rho}{2} v_n z_v + \mu\partial_n z_v + z_p n)\cdot[v_h]| \leq ch^2.$$

□

We immediately get:

Theorem 5. *Under the assumptions (17), (18) and (19), one has that*

$$|J(u) - J^{\mathrm{NS}}(u_h)| \leq c\, h^2.$$

References

[1] I. Babuška, A. Miller, *The post-processing approach in the finite element method-part 1: Calculation of displacements, stresses and other higher derivatives of the displacements*, Int. J. Numer. Meth. Engng. 20 (1984), 1085-1109.

[2] S. Badia, R. Codina, *Unified stabilized finite element formulations for the Stokes and the Darcy problems*, SIAM J. Numer. Anal. 47 (2009), 1971-2000.

[3] Y. Bazilevs, T.J.R. Hughes, *Weak imposition of Dirichlet boundary conditions in fluid mechanics*, Comput. & Fluids 36 (2007), 12-26.

[4] Y. Bazilevs, C. Michler, V.M. Calo, T.J.R. Hughes, *Isogeometric variational multiscale modeling of wall-bounded turbulent flows with weakly enforced boundary conditions on unstretched meshes*, Comput. Methods Appl. Mech. Engrg. 199 (2010), 780-790.

[5] R. Becker, *Mesh adaptation for Dirichlet flow control via Nitsche's method*, Commun. Numer. Methods Eng. 18 (2002), 669-680.

[6] R. Becker, M. Braack, *Solution of a stationary benchmark problem for natural convection with large temperature difference*, Int. J. Therm. Sci. 41 (2002), 428-439.

[7] R. Becker, D. Capatina, R. Luce, D. Trujillo, *Finite element formulation of general boundary conditions for incompressible flows*, Comput. Methods in Appl. Mech. Eng. 295 (2015), 240-267.

[8] R. Becker, D. Capatina, R. Luce, D. Trujillo, *Stabilized finite element formulation with domain decomposition for incompressible flows*, SIAM J. Sci. Comp. 37 (2015), 1270-1296.

[9] R. Becker, R. Rannacher, *An optimal control approach to a posteriori error estimation in finite element methods*. In *Acta Numerica*, A. Iserles (ed.), Cambridge Univ. Press (2001), 1-102.

[10] C. Bertoglio, A. Caiazzo, Y. Bazilevs, M. Braack, M. Esmaily, V. Gravemeier, A. Marsden, O. Pironneau, I. Vignon-Clementel, W. Wall, *Benchmark problems for numerical treatment of backflow at open boundaries*, Int. J. Numer. Methods Biomed. Eng. 34 (2018), doi:10.1002/cnm.2918.

[11] M. Braack, P.B. Mucha, *Directional Do-nothing Condition for the Navier-Stokes Equations*, J. Comput. Math. 32 (2014), 507-52.

[12] M. Braack, F. Schieweck, *Equal-order finite elements with local projection stabilization for the Darcy-Brinkman equations*, Comput. Methods Appl. Mech. Engrg. 200 (2011), 1126-1136.

[13] A. Brooks, T. Hughes, *Streamline upwind/Petrov-Galerkin formulations for convection dominated flows with particular emphasis on the incompressible Navier-Stokes equations*, Comput. Methods Appl. Mech. Engrg. 32 (1982), 199-259.

[14] C.-H. Bruneau, P. Fabrie, *New efficient boundary conditions for incompressible Navier-Stokes equations: a well-posedness result*, RAIRO Model. Math. Anal. Numer. 30 (1996), 815-840.

[15] E. Burman, M.A. Fernández, P. Hansbo, *Continuous interior penalty finite element method for Oseen's equations*, SIAM J. Numer. Anal. 44 (2006), 1248-1274.

[16] M. Crouzeix, P.A. Raviart, *Conforming and non-conforming finite elements for solving the stationary Stokes equations*, R.A.I.R.O. Anal. Numer. 7 (1973), 33-76.

[17] L.P. Franca, S.L. Frey, *Stabilized finite element methods. II: The incompressible Navier-Stokes equations*, Comput. Methods Appl. Mech. Engrg. 99 (1992), 209-233.

[18] T. Hoang, C.V. Verhoosel, F. Auricchio, E.H. van Brummelen, A. Reali, *Skeleton-stabilized isogeometric analysis: High-regularity interior-penalty methods for incompressible viscous flow problems*, Comput. Methods Appl. Mech. Engrg. 337 (2018), 324-351.

[19] T. Hoang, C.V. Verhoosel, C.-Z. Qin, F. Auricchio, A. Reali, E.H. van Brummelen, *Skeleton-stabilized immersogeometric analysis for incompressible viscous flow problems*, Comput. Methods Appl. Mech. Engrg. 344 (2019), 421-450.

[20] T. Hughes, L. Franca, M. Mallet, *A new finite element formulation for computational fluid dynamics. I: Symmetric forms of the compressible Euler and Navier-Stokes equations and the second law of thermodynamics*, Comput. Methods Appl. Mech. Engrg. 54 (1986), 223-234.

[21] V. John, G. Matthies, *Higher-order finite element discretizations in a benchmark problem for incompressible flows*, Int. J. Numer. Meth. Fluids 37 (2001), 885-903.

[22] V. John, *Reference values for drag and lift of a two-dimensional time-dependent flow around a cylinder*, Int. J. Numer. Meth. Fluids 44 (2004), 777-788.

[23] G. Nabh, *On high order methods for the stationary incompressible Navier-Stokes equations*, Interdisziplinäres Zentrum für Wiss. Rechnen der Univ. Heidelberg (1998), http://numerik.iwr.uni-heidelberg.de/Paper/Preprint1998-14.pdf

[24] J. Nitsche, *Über ein Variationsprinzip zur Lösung von Dirichlet-Problemen bei Verwendung von Teilräumen, die keinen Randbedingungen unterworfen sind*, Abh. Math. Univ. Hamburg 36 (1971), 9-15.

[25] R. Rannacher, S. Turek, *Simple nonconforming quadrilateral Stokes element*, Numer. Meth. Part. D.E. 8 (1992), 97-111.

[26] M. Schäfer, S. Turek, *The benchmark problem flow around a cylinder*. In *Flow Simulation with High-Performance Computers II*, Hirschel EH (ed.), Notes on Numerical Fluid Mechanics, vol. 52. Vieweg: Braunschweig (1996), 547-566.

[27] DFG benchmark 2D-2 (Re100, periodic)-Featflow. *http://www.featflow.de/en/benchmarks/cfdbenchmarking/flow/dfg_benchmark2_re100.html.*